Reprinted from ***Aircraft Engineering,*** *November 1956*

CoA Note No. 48

The College of Aeronautics

Four papers contributed by members of the staff and published on the occasion of the 10th anniversary of its foundation

Thermo-Elastic Formulae for the Analysis of Beams

Stress Distributions within a Structure due to Temperature Gradients and their Influence on Strength and Stiffness

By W. S. Hemp,* M.A., F.R.Ae.S.

THE kinetic heating associated with supersonic flight produces temperature gradients within the aircraft structure. These in their turn are responsible for so-called 'thermal stresses' in the components. The calculation of these effects falls into two stages. The first stage consists in the application of the theory of heat transfer to obtain the history of the temperature distribution in the structure. The second stage uses this data to obtain distributions of stress within the structure, resulting from these imposed temperature gradients and proceeds to assess their influence on strength and stiffness. The present paper is concerned entirely with this second stage of the problem and derives basic formulae for the analysis of beam-like structures and components. The results can be applied to wings, fuselages, etc., on the one hand, and to linear reinforcing members like stringers and longerons on the other, in the same way as the usual theories of bending and torsion are applied in the isothermal case.

The formulae obtained in this paper represent a generalization of the so-called engineering theory of bending and of the Wagner-Kappus torsion theory to include the effects of non-uniform temperature distribution. Kinematically, allowance is made for overall longitudinal extension, for curvature in two principal planes, for twist and for cross-sectional warping of the kind occurring in Saint Venant's torsion theory. Relationships between end load, bending moments and torques on the one hand and the kinematic parameters on the other are obtained, in a manner modelled on that of Ref. (1), by means of a 'Principle of Stationary Free Energy' established by the present writer in Ref. (2). These results, when combined with the well-known equilibrium equations for bending and torsion, constitute a complete theory of the problem under consideration. Applications to problems of stress analysis are indicated.

Concept of Free Energy

The work done by the external forces during an infinitesimal change of state of an elastic body is not in general a complete differential. This can only be asserted for the total energy transfer, which includes the heat supplied by the surroundings. However, in the case of 'isothermal' changes, it is shown in books on thermodynamics (for example, Ref. (3), Chap. XVI) that the work done is equal to the variation of a function of state termed the 'Free Energy'. Denoting a typical stress component by f, the corresponding strain component by e, the temperature rise from a reference state by θ and the free energy per unit volume by F, we can thus write for any infinitesimal volume element of a body

$$\Sigma f\delta e=\delta F, \text{ for } \delta\theta=0$$

or alternatively

$$(\partial F/\partial e)_\theta=f \qquad \ldots\ldots (1)$$

where Σ is a summation over all the relevant stress and strain components.

Eq. (1) may be used to calculate the free energy density F, apart from an additive function of θ, when the relations between stress and strain are known. We shall apply it here to a special case of stress distribution appropriate to the analysis of beams. A more general formula is given in Ref. (2).

Introducing a rectangular co-ordinate system 0 (x, y, z) and denoting stress and strain components by $f_{xx}, \ldots, f_{yz}, \ldots$ and $e_{xx}, \ldots, e_{yz}, \ldots$ we can write for the case when stresses 'transverse' to the axis 0z are zero the relations

$$\left.\begin{aligned} &f_{xx}=f_{yy}=0, f_{zz}=Ee_{zz}-E\alpha\theta \\ &f_{yz}=Ge_{yz}, \quad f_{zx}=Ge_{zx}, f_{xy}=0 \end{aligned}\right\} \qquad \ldots\ldots (2)$$

where E is Young's Modulus, G the shear modulus and α the coefficient of linear thermal expansion. Substituting from (2) in (1) and integrating we find

$$F=\tfrac{1}{2}Ee^2_{zz}+\tfrac{1}{2}G(e^2_{yz}+e^2_{zx})-Ee_{zz}\theta+F_0(\theta) \qquad \ldots\ldots (3)$$

where F_0 is an unknown function of θ, whose value is of no interest in the present application. It is to be remarked that F reduces, as it should, to the usual formula for 'strain energy density' when $\theta=0$.

Principle of Stationary Free Energy

Consider an elastic body subjected to given external forces and geometric constraints and in a state of non-uniform temperature distribution. Impose upon it a virtual displacement consistent with the geometric constraints. The resulting change in the sum of the free energy stored in the body and the potential energy of the external forces will, to the first order of small quantities, be zero.

If we give the external potential energy the perfectly correct, if a little unusual, name of free energy, we can write:

The total free energy of the body and the external force system is stationary for variations of the displacement, consistent with the geometric constraints, with the stipulation that the external forces and the temperature distribution are held constant during the variation ..... (4)

A formal proof of theorem (4) is given in Ref. (2).

Specification of Beam Deformation

Consider a uniform beam referred to an axis system 0 (x, y, z) as in FIG. 1. The line 0z is the axis of centroids of sections and 0x, 0y are parallel to the principal axes of the sections. This implies that

$$\iint x\,dx\,dy=\iint y\,dx\,dy=\iint xy\,dx\,dy=0 \qquad \ldots\ldots (5)$$

The displacement components at any point of the beam are denoted by (u, v, w). Then the elementary theory of beams supplemented by an allowance for torsional warping is expressed, after the manner of Ref. (1), by the following equations:

$$\left.\begin{aligned} u&=U(z)-y\chi(z) \\ v&=V(z)+x\chi(z) \\ \omega&=W(z)-x(dU/dz)-y(dV/dz)+\phi(x,y)(d\chi/dz) \end{aligned}\right\} \qquad \ldots\ldots (6)$$

The quantities (U, V, W) define a translation of normal sections, which, in accordance with the assumptions of beam theory, also rotate as rigid lamina with components ($-dV/dz$, dU/dz, χ). The final term in w gives the warping associated with the twist $d\chi/dz$ expressed by means of Saint Venant's torsion function ϕ,* where the additive constant, normally left undetermined in ϕ, is fixed by the relation

$$\iint \phi\,dx\,dy=0 \qquad \ldots\ldots (7)$$

Introducing the flexural centre with co-ordinates (x_F, y_F) given by

$$x_F=-\frac{1}{I}\iint y\phi\,dx\,dy,\ y_F=\frac{1}{I'}\iint x\phi\,dx\,dy \qquad \ldots\ldots (8)$$

where

$$I=\iint y^2\,dz\,dy,\ I'=\iint x^2\,dx\,dy \qquad \ldots\ldots (9)$$

we can introduce displacement components (U_F, V_F) of the flexural axis by

$$U_F=U-y_F\chi,\ V_F=V+x_F\chi \qquad \ldots\ldots (10)$$

and so replace (6) by

$$\left.\begin{aligned} u&=U_F-(y-y_F)\chi \\ v&=V_F+(x-x_F)\chi \\ \omega&=W-x(dU_F/dz)-y(dV_F/dz)+\phi_F(d\chi/dz) \end{aligned}\right\} \qquad \ldots\ldots (11)$$

where

$$\phi_F=\phi-xy_F+yx_F \qquad \ldots\ldots (12)$$

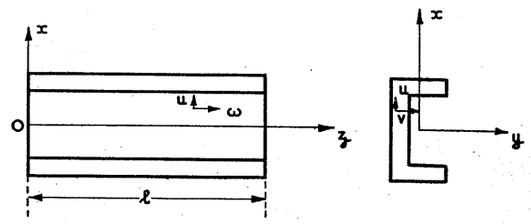

Fig. 1

REFERENCES TO LITERATURE

(1) G. Y. Dzhanelidze. *On the Theory of Thin and Thin-walled Rods.* (N.A.C.A. Tech. Memo. 1309.)

(2) W. S. Hemp. 'Fundamental Principles and Theorems of Thermo-Elasticity.' *Aero Quart. VII*, August 1956.

(3) J. K. Roberts. *Heat and Thermodynamics.* (Blackie, Fourth Edition, 1951.)

(4) A. E. H. Love. *Mathematical Theory of Elasticity.* (Cambridge, 1934.)

(5) R. L. Bisplinghoff. 'Some Structural and Aero-elastic Considerations of High Speed Flight.' *J. Ae. Sc.*, Vol. 23, No. 6, June 1956.

* Professor of Aircraft Structures and Aero-Elasticity, College of Aeronautics, Cranfield.

* Ref. 4 § 216.

Eqs. (5), (7), (8) and (9) show that ϕ_F defined by (12) satisfies the relations

$$\iint \phi_F dxdy = \iint x\phi_F dxdy = \iint y\phi_F dxdy = 0 \quad \ldots\ldots (13)$$

Assuming that the displacements are small, we can now derive from (11) formulae for the strain components e_{zz}, e_{zx} and e_{yz}. We find

$$e_{zz} = \partial w/\partial z = \epsilon - x\kappa' + y\kappa + \phi_F\omega \quad \ldots\ldots (14)$$

where

$$\epsilon = dW/dz,\ \kappa = -d^2V_F/dz^2,\ \kappa' = d^2U_F/dz^2,\ \omega = d^2\chi/dz^2 \quad \ldots\ldots (15)$$

and

$$\left.\begin{aligned} e_{zx} &= (\partial u/\partial z) + (\partial w/\partial x) = \tau\{(\partial\phi_F/\partial x) - (y - y_F)\} \\ e_{yz} &= (\partial w/\partial y) + (\partial v/\partial z) = \tau\{(\partial\phi_F/\partial y) + (x - x_F)\} \end{aligned}\right\} \quad \ldots\ldots (16)$$

where

$$\tau = d\chi/dz \quad \ldots\ldots (17)$$

The quantity ϵ is the average longitudinal strain, κ and κ' are the components of bending curvature of the flexural axis, τ is the twist and ω the rate of twist. It can be shown that (14) and (16) are still valid, even for the case of large deflexions, if the beam is thin and ϵ, κ, κ', τ and ω are appropriately defined. See, for example, Ref. (4), Chap. XVIII, Eq. (18) and footnote.

Formula for the Free Energy in a Beam

Neglecting as is usual in beam theory the transverse stress components f_{xx}, f_{yy} and f_{xy}, we can now use Eq. (3) for F, substituting from (14) and (16), to obtain a formula for the total free energy $\mathcal{F}$ stored in a length l of a beam.

Carrying out the necessary calculations and restricting ourselves to the case where E, G and α are independent of the temperature and are therefore constant, we find

$$\begin{aligned} \mathcal{F} = \int_0^l [&\tfrac{1}{2}E(A\epsilon^2 + I\kappa^2 + I'\kappa'^2 + \Gamma\omega^2) + \tfrac{1}{2}C\tau^2 \\ &- E(A\epsilon_\theta\epsilon + I\kappa_\theta\kappa + I'\kappa'\kappa'_\theta + \Gamma\omega_\theta\omega)]dz \\ &+ \text{a constant} \end{aligned} \quad \ldots\ldots (18)$$

where

$$\left.\begin{aligned} A &= \iint dxdy,\ \Gamma = \iint \phi_F^2 dxdy \\ C &= G\iint[\{(\partial\phi_F/\partial x) - (y - y_F)\}^2 + \{(\partial\phi_F/\partial y) + (x - x_F)\}^2]dxdy \end{aligned}\right\} \quad (19)$$

and

$$\left.\begin{aligned} \epsilon_\theta &= (\alpha/A)\iint\theta dxdy \\ \kappa_\theta &= (\alpha/I)\iint y\theta dxdy \\ \kappa_\theta' &= -(\alpha/I')\iint x\theta dxdy \\ \omega_\theta &= (\alpha/\Gamma)\iint\phi_F\theta dxdy \end{aligned}\right\} \quad \ldots\ldots (20)$$

The quantity A is the cross-sectional area, Γ is the torsion-bending constant and C is the Saint Venant torsional rigidity. The quantity ϵ_θ is the mean longitudinal thermal strain, κ_θ and κ_θ' may be termed the thermal curvatures and ω_θ the thermal rate of twist. The temperature enters our theory via these last four quantities.

Virtual Work of the External Forces

Let the external forces per unit length acting on the beam be denoted by (X, Y, Z) (see FIG. 2). The components (X, Y) are assumed to act on the flexural axis, while Z is located on the axis of centroids. Let Θ be the externally applied torque per unit length. The equations of equilibrium can then be written as

$$\left.\begin{aligned} &(dS/dz) + X = 0,\ (dS'/dz) + Y = 0,\ (dP/dz) + Z = 0 \\ &(dM/dz) - S' = 0,\ (dM'/dz) + S = 0,\ (dT/dz) + \Theta = 0 \end{aligned}\right\} \quad \ldots\ldots (21)$$

where S, S' are the shear forces in the directions $0x$, $0y$ assumed to act at the flexural centre, P is the end load acting along the axis of centroids, M and M' are the bending moments about the principal axes and T is the torque. The sign convention implied by (21) is illustrated in FIG. 3.

Multiplying the first three of (21) by δU_F, δV_F and δW and the last by $\delta\chi$, adding and integrating dz from 0 to l, we find

$$\begin{aligned} &\int_0^l (X\delta U_F + Y\delta V_F + Z\delta W + \Theta\delta\chi)dz \\ &\quad = \int_0^l \{-(dS/dz)\delta U_F - (dS'/dz)\delta V_F - (dP/dz)\delta W - (dT/dz)\delta\chi\}dz \\ &\quad = [-S\delta U_F - S'\delta V_F - P\delta W - T\delta\chi]_0^l \\ &\quad\quad + \int_0^l \{S\delta(dU_F/dz) + S'\delta(dV_F/dz) + P\delta\epsilon + T\delta\tau\}dz \end{aligned}$$

where we have integrated by parts and used (15) and (17). Substituting for S and S' from (21) and integrating by parts once more we find

$$\begin{aligned} &\int_0^l (X\delta U_F + Y\delta V_F + Z\delta W + \Theta\delta\chi)dz \\ &\quad + [S\delta U_F + S'\delta V_F + P\delta W - M\delta(dV_F/dz) + M'\delta(dU_F/dz) + T\delta\chi]_0^l \\ &\quad = \int_0^l (P\delta\epsilon + M\delta\kappa + M'\delta\kappa' + T\delta\tau)dz \end{aligned} \quad \ldots\ldots (22)$$

The left-hand side of (22) is the required virtual work of the external forces. In making this statement we are implying certain assumptions as to their distribution over the section, but this is in accordance with the spirit of beam theory, which cannot of course really allow for variations of this kind.

Variational Equation of Equilibrium and Load-Deformation Relations

We are now in a position to apply the theorem of (4) to our problem. Remarking that the virtual work of (22) is equal to minus the increment of potential or free energy of the external forces, we can write

$$\delta\mathcal{F} = \int (P\delta\epsilon + M\delta\kappa + M'\delta\kappa' + T\delta\tau)dz \quad \ldots\ldots (23)$$

Substituting from (18) into (23) yields

$$\begin{aligned} &\int_0^l (P\delta\epsilon + M\delta\kappa + M'\delta\kappa' + T\delta\tau)dz = \int_0^l \{EA(\epsilon - \epsilon_\theta)\delta\epsilon + EI(\kappa - \kappa_\theta)\delta\kappa \\ &\quad + EI'(\kappa' - \kappa'_\theta)\delta\kappa' + C\tau\delta\tau + E\Gamma(\omega - \omega_\theta)\delta\omega\}dz = [E\Gamma(\omega - \omega_\theta)\delta\tau]_0^l \\ &\quad + \int_0^l (EA(\epsilon - \epsilon_\theta)\delta\epsilon + EI(\kappa - \kappa_\theta)\delta\kappa + EI'(\kappa' - \kappa'_\theta)\delta\kappa' \\ &\quad + [C\tau - d\{E\Gamma(\omega - \omega_\theta)\}/dz]\delta\tau)dz \end{aligned}$$

Where we have written $\delta\omega = d(\delta\tau)/dz$ and integrated by parts. We deduce by comparison of the first and last terms of this variational equation that

$$\left.\begin{aligned} P &= EA(\epsilon - \epsilon_\theta) \\ M &= EI(\kappa - \kappa_\theta) \\ M' &= EI'(\kappa' - \kappa'_\theta) \\ T &= C\tau - d\{E\Gamma(\omega - \omega_\theta)\}/dz \end{aligned}\right\} \quad \ldots\ldots (24)$$

Notation

(x, y, z) = Rectangular cartesian co-ordinates
(x_F, y_F) = Co-ordinates of flexural centre
l = Length of beam
A = Area of section of beam
Γ = Torsion-Bending Constant
I, I' = Second moments of area of beam section about principal axes through centroid
(u, v, w) = Displacement components
(U, V, W) = Components of translation of normal sections of beam
(U_F, V_F) = Displacement components at flexural axis
χ = Torsional rotation angle
e = Strain component
$(e_{xx}, \ldots e_{yz}, \ldots)$ = Strain components referred to co-ordinates (x, y, z)
ϵ = Average longitudinal strain
κ, κ' = Components of curvature of the flexural axis
τ = Twist
$\omega = d\tau/dz$ = Rate of twist
E = Young's Modulus
G = Shear Modulus
α = Coefficient of linear expansion
C = Saint Venant torsional rigidity
f = Stress component
$(f_{xx}, \ldots, f_{yz}, \ldots)$ = Stress components, referred to co-ordinates (x, y, z)
P = Tensile end load in beam, acting along line of centroids
M, M' = Bending moments, taken about principal axes through the centroid
T = Torque about flexural axis
S, S' = Shear forces located at flexural centre
$(X, Y, Z,)$ = Components of external forces per unit length of beam, with (X, Y) located at the flexural axis and Z acting along the line of centroids
Θ = Externally applied torque per unit length taken about flexural axis
θ = Temperature rise from a reference state of zero stress and strain
F = Free energy per unit volume
F_0 = Value of free energy at zero strain
$\mathcal{F}$ = Total free energy
ϕ = Saint Venant's torsion function
ϕ_F = Ditto referred to flexural axis
ϵ_θ = 'Thermal longitudinal extension'
$\kappa_\theta, \kappa'_\theta$ = 'Thermal curvatures of the flexural axis'
ω_θ = 'Thermal rate of warping'

and at the ends $z=0, l$.

$$\left.\begin{array}{l}\text{Either } \tau, \text{ that is to say the warping, given}\\ \text{or } \omega=\omega_\theta\end{array}\right\} \quad \ldots\ldots\ldots\ldots \quad (25)$$

Eqs. (24) give the required load-deformation relations, while (25) gives special boundary conditions. The first three of (24) may be verified using (14) and (2), but the formula for T and (25) can only be obtained from the variational process, because of the approximate character of the theory. The relations (24) show that the usual isothermal formulae can be applied to the case of non-uniform temperature, so long as we first subtract what we have called the thermal extensions, curvatures and rates of warping from the 'true' values of these quantities. It is to be remarked that there is no 'thermal twist'. This is due to the fact that in an isotropic body, such as we are considering here, the thermal effects produce no shear strain.

Stress Analysis

It is of course quite clear that Eqs. (24) together with the usual equations of static equilibrium will enable us, in a familiar way, to analyse the deformation of beams and to calculate the stresses which occur in them for the case where the beam is in a state of non-uniform temperature. Consider, as an example, the case of an unloaded cantilever. Eqs. (24) with $P=M=M'=T=0$ and Eqs. (25) give

$$\epsilon=\epsilon_\theta,\ \kappa=\kappa_\theta,\ \kappa'=\kappa'_\theta,\ C\tau-E\Gamma(d^2\tau/dz^2)+E\Gamma(d\omega_\theta/dz)=0 \quad \ldots\ldots \quad (26)$$

and

$$(\tau)_{z=0}=0,\ (\omega-\omega_\theta)_{z=l}=0 \quad \ldots\ldots\ldots\ldots\ldots\ldots\ldots\ldots \quad (27)$$

Use of (15) and (17) in conjunction with these equations will enable a deflexion analysis to be carried out. Again Eqs. (14) and (16) combined with (2), will in conjunction with (26), (27) yield formulae for stresses. For example, the direct stress f_{zz} is given by

$$f_{zz}=E(\epsilon_\theta-x\kappa'_\theta+y\kappa_\theta+\phi_P\omega)-E\alpha\theta \quad \ldots\ldots\ldots\ldots\ldots\ldots \quad (28)$$

where $\omega=d\tau/dz$ is obtained by integrating (26). The shear stresses f_{zx}, f_{yz} obtained in a similar way are only those due to torsion. More accurate results can be obtained for thin-walled sections by using (28) and the usual membrane equilibrium equations for shells.

Buckling Problems

Many problems of buckling due to initial thermal stresses may be solved by use of the customary formulae. The present investigation yields as in the last section values of end load, bending moments and torque carried by members due to temperature gradients. These may be used in conjunction with equilibrium equations, written down for the deflected state, to calculate critical loads and the corresponding temperature states which will give rise to buckling. This is quite a standard procedure and the well-known formulae for flexural and torsional buckling loads may be used. However, more subtle effects can arise, which because of their non-linear character are outside the scope of the present paper. Reference may be made to a paper by Bisplinghoff (Ref. (5)), where the effects of initial thermal stresses on torsional stiffness are considered. We confine ourselves here to quoting, without proof, a generalization of the last of (24). This may be written

$$T=\{C+\iint f_{zz}(x^2+y^2)dxdy\}\tau-d\{E\Gamma(\omega-\omega_\theta)\}/dz \quad \ldots\ldots\ldots\ldots \quad (29)$$

where f_{zz} are initial stresses. It is easily shown that the double integral may be negative in practical cases and so lead to a reduction of torsional stiffness and a consequent danger of buckling or other undesirable effects. A re-examination of the theory of large deflexions of beams would appear to be desirable.

Fig. 2

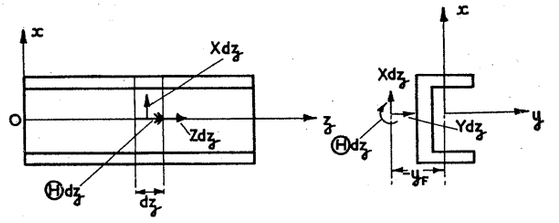

Fig. 3

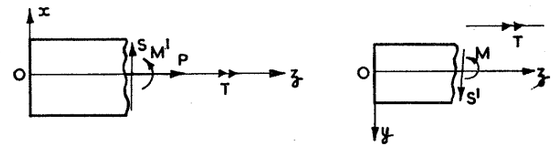

Some Aspects of Turbojet Performance Calculation at High Flight Mach Numbers

Problems of Performance Prediction in Truly Supersonic Engines

By J. R. Palmer,* M.A., A.F.R.Ae.S.

AT the present time turbojet aircraft types which are capable of level flight Mach numbers well into the supersonic range are appearing in increasing numbers. Yet, while this represents in a sense a new phase in the evolution of piloted aircraft, from the point of view of the propulsion engineer it is rather the end of an era, in that hitherto the turbojet engines employed have been essentially subsonic engines suitably strengthened. Henceforth we may expect to see the use of engines specifically designed for the appropriate range of Mach number, and it is the purpose of this article to review some of the implications of this change of outlook in so far as they affect the prediction of engine performance.

The Choice of Type of Power Plant

In a paper already firmly established as a classic, Moult[1] has considered the major types of engine relevant to the range up to Mach 3, and makes it very clear that the correct choice of type must depend on a detailed analysis of the aircraft power requirements over its whole flight path. The optimum power plant varies widely with the different Mach numbers and altitudes encountered, and consequently a knowledge of the operational requirements of the aircraft, dictating as they do the relative importance in terms of time of these various speeds and altitudes, is indispensable to a full evaluation of the engine problem. As will be shown, however, the trend is towards variable engine geometry, so that the 'single design point' engine with which we have hitherto been familiar may be expected to give way to a type which, even if it cannot be correctly matched to all the aircraft requirements, can at least be controlled in such a way as to achieve a considerable measure of variability of its design point.

Subject to these considerations, it is now proposed to restrict consideration to the turbojet engine, it being assumed that the aircraft requirement is such as to make the choice of this type of unit appropriate.

* Senior Lecturer, Department of Aircraft Propulsion, College of Aeronautics, Cranfield.

REFERENCES TO LITERATURE

(1) E. S. Moult. *Power Plants for Supersonic Flight.* (Fifth International Conference of R.Ae.S. and I.A.S., Los Angeles, 1955.)

(2) J. Hodge. *Gas Turbines. I—Cycles and Performance Estimation.* (Butterworth. 1955.)

(3) D. Fielding and J. E. C. Topps. *Thermodynamic Properties of Air and Combustion Products o Hydrocarbon Fuels, Parts I, II and III.* (N.G.T.E. Reports Nos. R.74 (June 1950), R.120 (July 1952) and R.160 (June 1954)).

(4) J. H. Keenan and J. Kaye. *Gas Tables.* (Wiley. 1948.)

(5) J. Seddon. *Air Intakes for Aircraft Gas Turbines*—J.R.Ae.S. (October, 1952.)

(6) D. D. Wyatt. *An Analysis of Turbojet-Engine-Inlet Matching.* (N.A.C.A. Technical Note 3012, September, 1953.)

(7) A. W. Morley. *Aircraft Propulsion—Theory and Performance.* (Longmans, 1953.)

The Design Mach Number

In view of the preceding remarks, a supersonic turbojet may not have a unique design point: however, the aerodynamic and mechanical design will tend to become increasingly difficult with increase of Mach number, so that for convenience we may define the design Mach number as the highest value at which it is intended to operate the engine. In this connexion it is very important to appreciate how severely the engine operating conditions change with Mach number in the range Mach 2 to 3, the latter value being the highest which it is proposed to consider here.

TABLE I shows that at the upper end of the range a change of 0·5 in Mach number more than doubles the free stream total pressure, while the total temperature increases by about 100 deg. C. Owing to intake losses, these pressures are not fully achieved within the engine, nor are the metal temperatures as high as those of the air, but it is apparent that quite small changes in flight Mach number can lead to radical increases in the mechanical loading of the engine, accompanied by a serious rise in metal temperatures (with consequent deterioration of their mechanical properties) at the nominally 'cold' end.

Effect of Specific Heat Variation

Hitherto it has been common practice to evaluate turbojet performance on the basis of fixed specific heats, different values being taken in the various parts of the cycle appropriate to the general temperature level and, in the case of the expansion, to the fuel-air ratio employed. Pressure changes are then determined by employing adiabatic or polytropic efficiencies based on temperature changes, together with the constant specific heat isentropic law $P/T^{\gamma/(\gamma-1)}$=constant, where the specific heat ratio γ is related to the gas constant R and the specific heat C_p at constant pressure by the equation $\gamma=C_p/(C_p-R)$.

It has been shown[2, 3] that for moderate changes of temperature and pressure (of the order of 200 deg. C. in the case of temperature), such a procedure yields no serious error: an appropriate mean value of C_p is the true specific heat at the arithmetic mean temperature of the process considered. However, temperature and pressure changes of the magnitude shown in TABLE I for the higher Mach numbers are far from moderate, and even larger changes occur across the propelling nozzle, consequently accurate performance calculation can no longer be based on the familiar elementary isentropic relations, but must take account of the continuous variation of gas specific heats. Changes in enthalpy rather than temperature must be considered, the efficiencies employed must be similarly based, and the appropriate form of the isentropic law is now $R\log_e(P_2/P_1)=\int_1^2(C_p/T)dT$.

The appropriate thermodynamic data are of course, available in convenient graphical or tabular form[3, 4], but the whole process of cycle calculation is considerably slowed up. In what follows, numerical calculations have in general been made using mean specific heat values, with the exception of TABLE I, since the object is to illustrate trends and procedures rather than to produce design data. Such data are in any case critically dependent on the numerical values assumed for efficiencies and losses, but the need for more sophisticated methods in practical performance calculation must be constantly borne in mind.

Design Point Performance

In deciding the layout of a simple turbojet without reheat to meet a certain design point specification in terms of flight altitude and Mach number, the designer has at his disposal the two variables, turbine inlet temperature and compressor pressure ratio. As is well known (see FIG. 1), the effect of increasing turbine inlet temperature at constant pressure ratio is to increase the specific thrust, owing to the increase of jet velocity, but there is a certain value of this temperature for which the specific fuel consumption is a minimum. Though this optimum temperature increases with flight Mach number, it is lower than values currently attainable (Ref. 1, FIG. 14). If the compressor pressure ratio is increased at constant turbine inlet temperature, the specific thrust at first increases and the specific fuel consumption falls off: at a certain 'thrust-optimum' pressure ratio the specific thrust reaches a maximum, though the specific fuel consumption is still decreasing. Ultimately a 'consumption-optimum' pressure ratio is reached at which the specific fuel consumption reaches a minimum. Further increase of pressure ratio beyond this value would be pointless, since the specific thrust and fuel consumption both deteriorate. The values of sea level static pressure ratio at which these two optima are reached decrease markedly with increase of flight altitude and Mach number.

The above remarks apply to the turbojet without reheat, and lead to the conclusion that for a given turbine inlet temperature, which will tend to be as high as possible, a quite moderate sea level static pressure ratio will suffice to strike an acceptable balance between specific thrust and fuel consumption.

While the same general trends are observable in the case of the reheated engine, there are certain important differences to be noted. If the reheat temperature is fixed at the highest attainable value, the highest possible turbine inlet temperature is desirable from the point of view of both thrust and fuel consumption, since in this way the maximum permissible proportion of the total fuel is burnt at high pressure, leading to maximum thermal efficiency. As regards the effect of compressor pressure ratio, the values of TABLE II show that even at a sea level static pressure ratio of 12 the specific thrust and fuel consumption are both improving. The reason for this is that increase of compressor pressure ratio raises the pressure ratio available across the propelling nozzle, and since the jet pipe total temperature is held constant, the jet velocity also rises. In the unreheated case, however, the jet pipe total temperature falls with increase of pressure ratio, tending to counteract the rise of jet velocity: below the thrust-optimum pressure ratio referred to above, the nozzle pressure ratio effect predominates and the jet velocity rises, while above the optimum the temperature effect prevails and the jet velocity falls.

TABLE I

Free Stream Total Conditions at Various Flight Mach Numbers in the Stratosphere

Mach Number ...	0	0·5	1·0	1·5	2·0	2·5	3·0
Total Temperature (°K)	216·5	227·3	259·9	314·1	389·9	486·2	601·6
Total Pressure / Static Pressure ...	1·000	1·186	1·894	3·667	7·842	17·16	37·03

TABLE II

Effect of Compressor Pressure Ratio on Specific Thrust and Fuel Consumption at Mach 2·5 in the Stratosphere

Turbine Inlet Total Temperature 1400 deg. K.

Pressure Ratio (S.L.S.)		4	6	8	10	12
Specific Thrust (lb. sec./lb.)	Unreheated ...	47·7	46·6	45·3	44·0	42·7
	Reheated	79·8	81·5	82·4	83·0	83·4
Specific Fuel Consumption (lb./lb. hr.)	Unreheated ...	1·59	1·51	1·45	1·40	1·37
	Reheated	2·09	2·05	2·02	2·00	1·98

TABLE III

Relative Thrusts and Exit Diameters of Convergent and Convergent-Divergent Nozzles

(Constant Mass Flow and Inlet Total Temperature)

Design Overall Total-to-Static Pressure Ratio		1·83	3	5	10	20	30	40	50	∞
Gross thrust Relative to Convergent Nozzle at Pressure Ratio of 1·83	Convergent	1·00	1·30	1·49	1·63	1·70	1·72	1·73	1·74	1·77
	Convergent-Divergent ...	1·00	1·31	1·54	1·78	1·96	2·04	2·10	2·14	2·77
Ratio of Exit Diameters Convergent-Divergent / Convergent ...		1·00	1·06	1·18	1·44	1·79	2·04	2·26	2·41	∞

While such design point data are an essential preliminary to the choice of engine design parameters, they are by no means conclusive. As the design flight Mach number rises, the importance of assessing the performance of the installation as a whole increases also. In the first place, it is evident from the figures of TABLE II that even on thermodynamic grounds alone a very different choice of engine design parameters will be made according as reheat is employed or not. Now while the reheated engine has the higher specific thrust, and hence the lower frontal area and (probably) weight for a given thrust, its greater fuel consumption will count increasingly against it as the aircraft range requirement increases. But it does not necessarily follow that the changeover from a reheated to an unreheated engine will occur at some fairly definite range or endurance, since the proposed aircraft application will dictate the proportion of flying time spent at or near the maximum Mach number. This raises considerations of flight path planning which cannot be entered into in a discussion of this nature.

While the requirements for long-range supersonic aircraft are not yet sufficiently clear to determine the relative merits of the two forms of engine, for present short-range applications the tendency is towards the reheated engine. Hitherto reheat has been designed 'on to' existing engines rather than 'into' new ones, but the conflict in choice of pressure ratio indicates that from the performance viewpoint there is much to be said for selecting the engine cycle with reheat as an integral part.

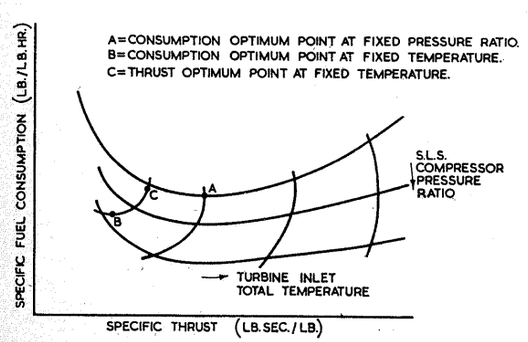

Fig. 1.—The effect of compressor pressure ratio and turbine inlet temperature on specific thrust and fuel consumption at constant flight speed and altitude

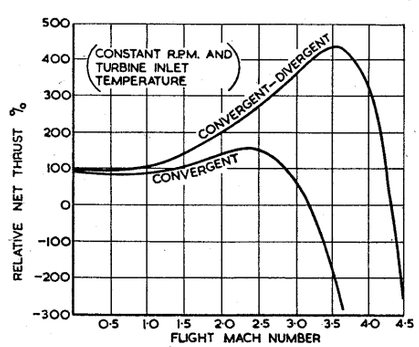

Fig. 2.—Variation with flight Mach number of net thrust of engines with convergent and convergent-divergent nozzles

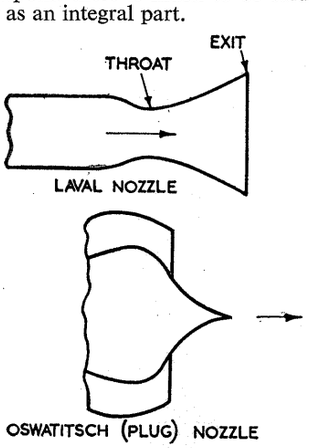

Fig. 3.—Laval and Oswatitsch nozzles

Consideration must be given to the installation as a whole for another very important reason: for while engine performance calculations may indicate a certain optimum choice of compressor pressure ratio and, to a lesser extent, of turbine inlet and reheat temperatures, the relative sizes of the major engine components also depend on these parameters. In particular, a low temperature or low pressure ratio engine requires a relatively larger combustion and reheat system than one designed for higher values, due to the low gas velocities in those components. Thus a low design pressure ratio, which is desirable in an unreheated engine from the point of view of specific thrust, may lead to unfavourable dimensional matching of the components, which can only be remedied by increasing the design pressure ratio above the thermodynamic optimum. What constitutes the optimum envelope shape of the engine is perhaps open to debate, since this must depend on, amongst other things, whether a submerged or podded installation is intended. Hitherto the tendency has been to regard the 'tubular' engine, of relatively constant diameter at all stations, as the ideal, but as will be seen, high Mach number engines tend to require a large nozzle exit area owing to the high expansion pressure ratios developed. Thus it may be that an engine envelope of frustro-conical shape may come to be regarded as desirable, and this may well be in accordance with area rule requirements in the design of the aircraft. This latter is merely a particular aspect of the necessity for considering the 'thrust minus drag' of the installed engine rather than the thrust alone, since the dimensional matching of the bare engine will profoundly influence the shape—and thence the drag—of the nacelle or fuselage.

The Propelling Nozzle

In the essentially subsonic engines of the present day the final propelling nozzle is invariably of simple convergent form, for although the nozzle is fully choked, the loss in thrust due to insufficient expansion of the final jet has been regarded as less important than the gain in simplicity, lightness and compactness. But in a truly supersonic engine the pressure ratio across the propelling nozzle, of whose magnitude some indication has already been given, is so high that the loss in thrust due to under-expansion in a convergent nozzle is far too large to be acceptable, so that some form of convergent-divergent nozzle is indispensable in which the gas flow at least approaches full expansion. TABLE III gives some idea of the gain to be achieved by using a nozzle properly designed to give full expansion. Since the net thrust arises from the relatively small difference between the final jet velocity and the aircraft velocity—both of them large quantities in the flight regime we are considering—any loss in gross thrust is greatly magnified in its effect on the net thrust. FIG. 2 illustrates this, showing how with either a convergent or a convergent-divergent nozzle there is a certain Mach number at which the specific thrust peaks, and a higher Mach number at which the thrust vanishes due to the flight velocity becoming equal to the jet velocity. It is clear that the convergent-divergent nozzle provides a very substantial widening of the operating range available to the turbojet.

It is thus evident that a convergent-divergent nozzle is an inescapable necessity. As is well known, however, such nozzles are in general very inefficient when operated at pressure ratios below that for which they are designed, owing to shock losses and breakaway in the divergent portion. Consequently, to attain an acceptable level of engine efficiency over a reasonably wide range of flight speeds, continuous variation of the exit area will be an increasingly pressing need as the design Mach number increases, in order to match the nozzle to the available pressure ratio. To add to the difficulty of designing such a nozzle, it will normally be necessary to provide for at least a limited degree of throat area variation. For an engine intended to spend most of its working life with reheat in operation, a fixed throat area might be acceptable, as it would be for an unreheated engine, but normally one would need to retain at least a two-position throat, as used on present convergent nozzles, while the use of variable reheat to aid the matching of the various components might call for a throat area infinitely variable over quite wide limits. In recent years various schemes have been proposed for aerodynamic rather than mechanical variation of nozzle throat and/or exit area by injecting air at suitable points, but it seems unlikely that sufficient compressor bleed air—on which such systems depend—could be made available to attain the large area variations likely to be called for.

As shown by TABLE III, the exit diameter of the nozzle may tend to be the largest diameter of the engine if full expansion is catered for at the higher Mach numbers. While this may not be wholly undesirable, as indicated earlier, extremes of exit area would not be acceptable on grounds either of weight or of frontal area, so that the designer may be forced to tolerate some degree of under-expansion. The resulting thrust loss need not be large, however, and to some extent the necessity for such a 'cut-back' nozzle would entail the virtue of needing to cater only for a reduced range of exit area variation.

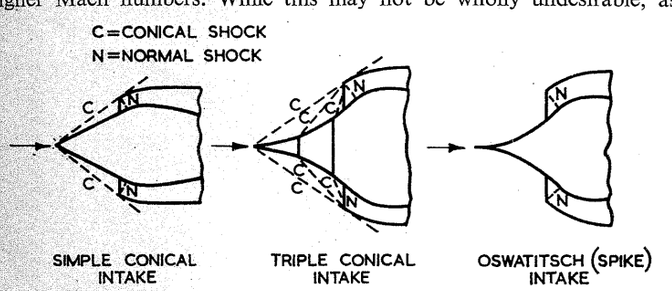

Fig. 4.—Types of centre-body intake

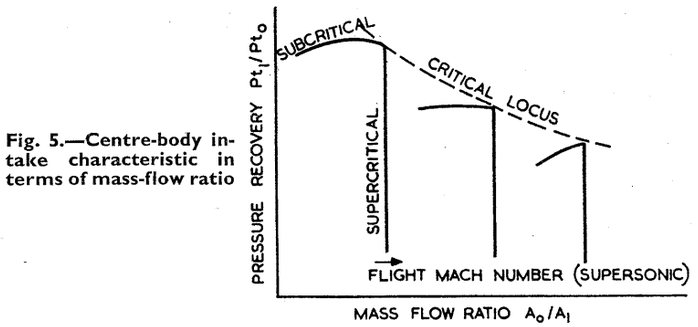

Fig. 5.—Centre-body intake characteristic in terms of mass-flow ratio

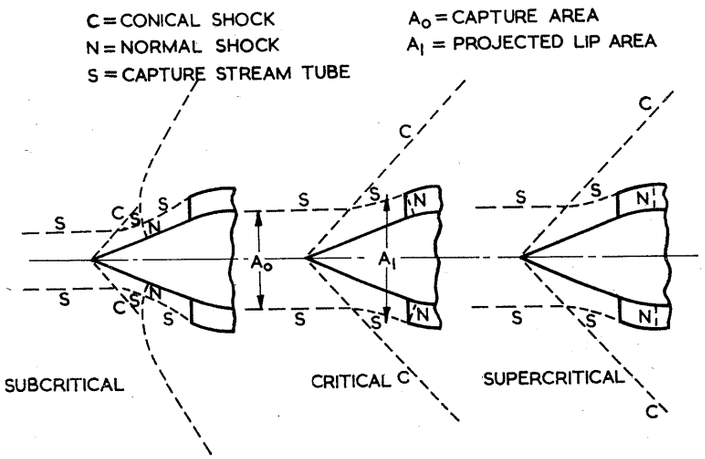

Fig. 6 (above).—Centre-body intake flow regimes

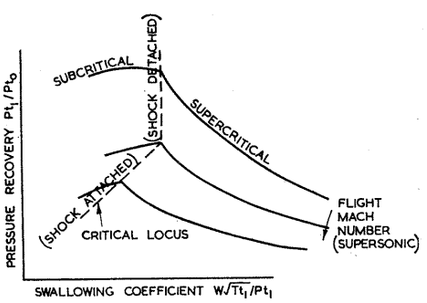

Fig. 7 (right).—Centre-body intake characteristic in terms of swallowing coefficient

While it would be hazardous to attempt to predict what forms these doubly variable nozzles may assume, at a time when a great deal of design and development effort can be presumed to be going into the solution of the problem, one may perhaps speculate on the possible revival of the Oswatitsch 'plug' type nozzle (see FIG. 3), with a centre-body designed to give isentropic expansion over a large pressure ratio. This type of nozzle has not found favour hitherto, since for full expansion it has a greater maximum diameter than the Laval type, but where a pronounced degree of under-expansion is designed for, the plug nozzle might well prove as efficient as a Laval nozzle of the same maximum diameter, while lacking the mechanical complications required by exit area variation. Throat area variation might be achieved by axial movement of the centre-body. Such a nozzle would, however, introduce its own problems in that the cooling of the centre-body would be very difficult.

The Intake

It has been said with some degree of truth that as the design Mach number increases, the front and back ends of the engine assume paramount importance, while the 'part in between' becomes of little account. Exaggerated though this view undoubtedly is, it is certainly true that the design of the intake, as of the propelling nozzle, becomes one of the major problems in successfully meeting a supersonic engine specification. The requirements are akin to those of the supersonic ramjet in that the intake losses have a major effect on the overall cycle efficiency, but whereas most ramjet applications involve a fairly narrow range of flight conditions at more or less constant peak temperature, for the turbojet the intake must perform efficiently over a wide range of Mach number at a variety of turbine inlet and reheat temperatures.

Now just as the single convergent nozzle performs adequately at subsonic and low supersonic flight speeds, so a simple pitot-type intake is reasonably efficient in this range. At subsonic speeds, provided only that the entry area is large enough to avoid choking, the pressure recovery (i.e. the ratio of the compressor inlet total pressure P_{t1} to the free stream total pressure P_{t0}) is only slightly dependent on forward speed and mass flow.[5] In the supersonic range, a normal shock forms which may be ahead of, at or behind the intake lip (subcritical, critical and supercritical states, respectively) according as the entry area is capable of passing an air mass flow greater than, equal to or less than the prevailing engine air requirement.

At Mach numbers greater than about 1·5, however, the pressure recovery of the simple pitot intake is unacceptably low owing to the large total pressure loss across the normal shock. It therefore becomes necessary to resort to some form of centre-body intake (see FIG. 4) in which the presence of a sharp-pointed body on the intake axis promotes the formation of a conical shock system whose pressure recovery is substantially better than that of the single normal shock associated with the pitot intake. A simple conical centre-body gives rise to a single conical shock while elaborating this to a polyconic body produces multiple conical shocks, the pressure recovery increasing with the number of shocks. In each case the conical shocks are followed by a normal shock which, in the critical state, is located at the intake lip. The ultimate development of the centre-body intake, previously mentioned in its reversed form as the plug-type nozzle, is the Oswatitsch ('spike') intake, in which the centre body has a continuous concave curvature, and the multiple shocks become a continuous band of infinitesimally weak compression waves impinging on the cowl lip: this leads to isentropic pressure recovery externally to the lip. However, all these types of intake must be followed by a subsonic duct connecting the cowl inlet to the compressor, and inevitably frictional losses occur in this duct even with an 'isentropic' centre-body. The degree of refinement in centre-body design to which it is worthwhile to go depends on the width of the range of operation over which high efficiency is required, since wide limits of operation require variation of all or any of lip area, centre-body position and centre-body nose angle, all of which are more difficult to achieve with the more elaborate types of centre-body.

The general characteristics of an intake with a simple conical centre-body are shown in FIG. 5, where the pressure recovery is plotted against the ratio of capture area (defined in FIG. 6) to projected lip area. This area ratio is sometimes referred to as the mass-flow ratio of the intake. In the subcritical region (see FIG. 6), the relationship between pressure recovery and mass-flow ratio, for given geometry and flight Mach number, depends on the detail design of the cowl lip, but generally the pressure recovery rises as the critical point is approached, reaching a maximum at or near the critical point. Once the supercritical region is entered the normal shock moves inside the cowl lip and increases in strength, leading to a fall in pressure recovery. At the same time the mass flow ratio stabilizes at the critical value, since the properties of the conical shock do not permit convergence of the capture stream tube behind the shock. As the flight Mach number increases, the critical mass-flow ratio increases slightly and the critical pressure recovery falls due to the increased strength of the shock system.

For the purpose of matching the intake characteristics to those of the rest of the engine, it is convenient to replot the intake performance curves in terms of the non-dimensional mass-flow (swallowing coefficient) $W\sqrt{(T_{t1}/P_{t1}}$ at the diffuser exit-compressor entry plane. FIG. 7 shows a characteristic presented in this form: it will be seen that for a given flight Mach number in the subcritical region the pressure recovery reaches a peak at or near the critical point. As the swallowing coefficient increases beyond the critical value, the pressure recovery decreases: it can be shown, in fact, that for supercritical operation the product of pressure recovery and swallowing coefficient is constant (see Ref. 6). It will be noted that up to a certain Mach number the critical swallowing coefficient is constant—this is the region where the conical shock is detached from the nose of the centre-body, leading to subsonic flow behind the shock and exactly sonic conditions at the cowl lip in the critical case. Once the conical shock is attached, the lip Mach number increases with that of the free stream, consequently the critical swallowing coefficient falls.

Three very important facts emerge from this review of the behaviour of the centre-body intake, though indeed they apply also to the pitot intake in the supersonic regime. Firstly, in the subcritical region the intake lip swallows less air than the shock system is capable of passing, so that the excess air is spilled externally, giving rise to an undesirable increase of drag and to unstable operation ('buzz') of the intake. Secondly, in the supercritical region the intake is operating at its limiting mass-flow ratio, i.e. it is no longer capable of passing whatever mass flow may be required by the engine. Thirdly, unless the conical shock is arranged to impinge upon the cowl lip, there will be a large drag associated with the spread of the shock outside the lip.

The question of matching the airflow capacities of the intake and engine will be considered shortly. Meanwhile it may be noted that in the interests of flow stability and drag reduction it is desirable to operate the intake in the supercritical state, though in order to minimize pressure losses the operating point should not be far removed from the critical. At the same time it is desirable to keep the conical shock impinging upon the cowl lip if possible, in order to reduce the external wave drag of the installation. Both these requirements indicate the desirability of a variable geometry intake.

Matching the Intake with the Remainder of the Engine

The procedure for determining the equilibrium running within the subsonic range of a simple turbojet of fixed geometry, with or without reheat, is by now well-known.[2,7] Briefly, the equilibrium of the engine is most easily visualized by considering first the compressor, combustion chamber and turbine alone (we may conveniently refer to these three components collectively as the 'turbocompressor'). Making due allowance for changes of mass flow through the system due to cooling air bleed and fuel addition, and for mechanical losses and mechanical power extraction, the characteristics of the individual components may be used with the three conditions of continuity of flow, compressor-turbine power balance and equality of rotational speeds to determine a unique relationship between the compressor operating point and the turbine inlet temperature (relative to compressor inlet temperature), as indicated in FIG. 8. This assumes that the geometry of the three components is fixed, other than compressor inlet guide vane rotation and/or blowoff governed by compressor operating conditions only: these latter can be accounted for in plotting the compressor characteristics.

Now this matching of the turbocompressor system implies a relationship between the air mass flow and the pressure ratio between compressor entry and turbine exit which depends upon the turbine inlet temperature. If we now take account of the characteristics of the final nozzle we find that since, for given throat area and reheat temperature the nozzle prescribes a relationship between mass flow and nozzle pressure ratio, the nozzle will limit the available range of operation of the turbocompressor to a family of operating lines whose position depends only on the ram ratio (i.e. the ratio of compressor inlet total pressure P_{t1} to ambient static pressure P_0), and which are coincident in the nozzle choking range (see FIG. 9). The effect of reducing the nozzle throat area at constant reheat temperature is to move the whole family of operating lines in the direction of reduced mass flow. Increase of reheat temperature at constant nozzle throat area has a similar effect, since this constitutes an increased blockage in the exhaust system equivalent to a decrease of throat area. Conversely, increase of throat area or decrease of reheat temperature moves the operating zone in the direction of increased mass flow. These trends are generally applicable, though certain forms of split-compressor engine, or engines with exceptionally low design pressure ratios, may not conform to them.

As with the intake, it is helpful to replot this characteristic of the turbocompressor-plus-jet pipe system to aid in matching these components

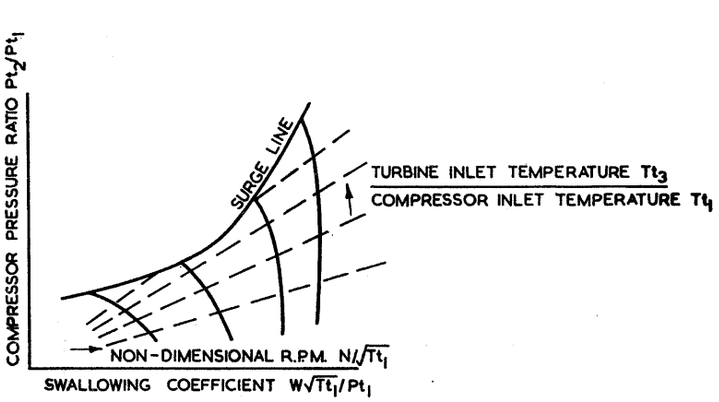

Fig. 8.—Turbocompressor characteristic

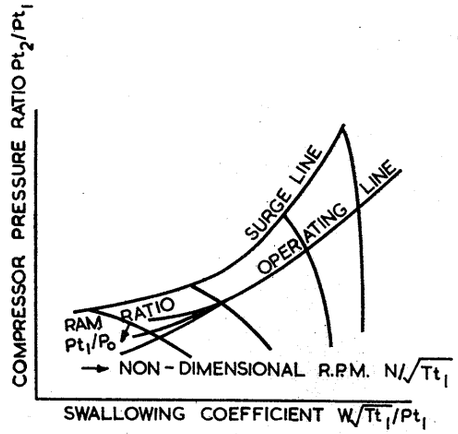

Fig. 9.—Characteristic of turbocompressor with propelling nozzle in terms of compressor pressure ratio

with the intake. For given engine rotational speed N and ambient static temperature, the values of $N/\sqrt{(T_{t1})}$ correspond to definite values of the free stream Mach number, since the compressor entry total temperature T_{t1} is equal to the free stream value T_{t0}. The corresponding values of free-stream total-to-static pressure ratio can then be calculated, enabling the value of the pressure recovery P_{t1}/P_{t0} (=Ram Ratio P_{t1}/P_0 divided by Free Stream Pressure Ratio P_{t0}/P_0) to be found for each point on the operating lines. This leads to a plot of pressure recovery against compressor inlet (diffuser exit) swallowing coefficient, as used for the intake characteristic, again with flight Mach number as parameter (see FIG. 10).

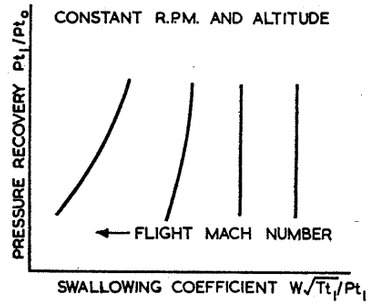

Fig. 10.—Characteristic of turbocompressor with propelling nozzle in terms of intake pressure recovery

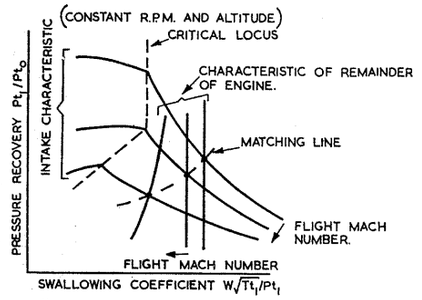

Fig. 11.—Determination of operating line by superimposition of characteristics of intake and of remainder of engine

We now have the characteristics of the intake and of the remainder of the engine plotted in terms of the same ordinate and abscissa. By superimposing the two characteristics (see FIG. 11), the equilibrium points can be found at various flight Mach numbers, for given rotational speed, altitude (which determines the ambient static temperature), reheat temperature and engine geometry. It is seen that the balance is such that the pressure recovery and swallowing coefficient both decrease with increase of Mach number. Whether increasing Mach number will move the operating point towards or away from the critical operating state of the intake depends on the relative slopes of the matching line and of the critical locus, except where the 'kink' in the critical locus occurs due to detachment of the conical shock.

It is seen, therefore, that it is in principle a straightforward operation to determine the performance of a supersonic turbojet, differing in degree only from the procedure for a subsonic engine, except as regards the matching of the intake with the rest of the engine. Two facts of great importance emerge from this. Firstly, it will generally be necessary to provide for variation of intake geometry (a threefold operation in its most general form, involving change of centre-body position, centre-body shape and cowl lip entry area), of nozzle throat and exit areas, and of the degree of reheat. It will not necessarily be essential to vary all these quantities, since in order to achieve mass flow balancing of the intake with the rest of the engine, variation of nozzle throat area or of reheat temperature could be as effective as changes in cowl entry area. Such changes of main engine operation will, however, tend to cause variation of the turbine inlet temperature, which may restrict their use, though the further complication of variable turbine nozzle guide vanes might be used to good effect in this connexion. The second consideration is that, with such a wealth of independently variable parameters (variable compressor stators are another addition to the list), the problem of adequately surveying the possible modes of operation of a proposed engine becomes formidable indeed. Practical considerations will doubtless tend to restrict the number of variables employed, but the best choice of control system must depend on exploring the characteristics of 'paper engines' in which full variability is available. It is fortunate for the performance engineer that techniques are being developed for using digital computers for such calculations.

REFERENCES TO LITERATURE

(1) A. J. Hearn. 'Conductivity induced by α particle bombardment.' *Phys. Rev.* 73, p. 1113, 1948.

(2) E. W. Saker *et al.* 'Indium antimonide as a flux meter material.' *Brit. Jou. of App. Phys.* 6, p. 217, 1955.

(3) I. M. Ross and E. W. Saker. 'Applications of indium antimonide.' *Jou. of Electronics* 1, p. 225, 1955.

(4) L. J. Giacoletto and J. O'Connell. 'A variable capacitance germanium junction diode for U.H.F.' *R.C.A. Rev.* 17, p. 69, 1956.

(5) P. Rappaport. 'The electron-voltaic effect in *p-n* junctions induced by β particle bombardment.' *Phys. Rev.* 93, p. 246, 1954.

(6) D. C. Brown and F. Henderson. Paper in preparation.

(7) R. F. Shea. *Principles of transistor circuits.* (John Wiley & Sons 1953.)

(8) J. G. Linvill and R. H. Mattson. 'Junction transistor blocking oscillator.' *Proc. I.R.E.* 43, p. 1632, 1955.

(9) J. E. Flood. 'Junction transistor trigger circuits.' *Wireless Eng.* 32, p. 122, 1955.

(10) J. N. Shive. 'Properties of germanium phototransistors.' *Jou. Opt. Soc. America* 43, p. 239, 1953.

(11) L. B. Gnagey. 'Determination of neutron intensity.' *Proc. I.R.E. Trans. Nuclear Science*, Vol. N.S.3, p. 11, 1956.

(12) D. C. Brown and B. P. Faraday. Paper in preparation.

The Possible Use of Semiconductor Devices in Aircraft

Possible Airborne Applications for a Range of New Materials with Unusual Properties

By D. C. Brown,* B.Sc., Ph.D., Dip.Ed.

SINCE the early years of the last decade a great deal of research has been done on the properties of the new class of materials called semiconductors because their electrical properties lie between those of conductors and insulators. Some of the results of these researches are described in this article, in particular those which are of interest to aircraft engineers. A simple explanation of the mechanism of these devices is given and some emphasis is laid on work done by staff and students of the Department of Aircraft Electrical Engineering at The College of Aeronautics.

Intrinsic or Pure Semiconductor material

The elements found in Group 4 of the periodic table of the elements, such as carbon, silicon and germanium, being tetravalent, form a very stable crystal lattice, FIG. 1. All the electrons in this crystal structure are closely associated with their parent atom and the minimum energy Q required to remove one of the electrons from this stable configuration is comparatively great.† The number of electrons per cubic centimetre, N, having the necessary energy to exist in the conduction band depends on the absolute temperature T and is given by $N=A \exp. (-Q/2KT)$, K being the Boltzmann constant. Thus at absolute zero the pure, or intrinsic, crystals of the Group 4 elements are insulators as there are no electrons in the conduction band. The energy gap Q varies from element to element and is ·76, 1·1 and 6 electron volts for germanium, silicon and carbon respectively.[1] The crystal of intrinsic germanium at room temperature has about 10^{13} electrons per cubic centimetre which can be compared to 10^{22} electrons per cubic centimetre for a typical metal. Intrinsic carbon with its very large energy gap is an almost perfect insulator, even at quite high temperatures, but with present day techniques it has not been possible to make diamonds.

All semiconducting materials exhibit the Hall effect to greater or lesser degree. That is, if an electric current is flowing in a crystal and a magnetic field is applied at right angles to the current flow, then a voltage appears across the crystal mutually at right angles to the applied electric and magnetic fields and proportional to the change in the magnetic field, FIG. 2. The magnitude of the voltage developed is proportional to the mobility of the carriers, which in intrinsic semiconductors are electrons. For germanium the mobility is 3,600 cms. per second in a field of 1 volt per centimetre.

Degenerate or Impure Semiconductor Material

If a few atoms from one of the Group 5 elements are introduced into the crystal lattice of one of the Group 4 elements (i.e. the crystal is doped with Group 5 impurities), then four of the five valence electrons of these impurity atoms will enter into the structure of the crystal, the fifth electron being bound to its parent atom by a field considerably reduced by the intervening crystal permittivity. FIG. 3 shows the effect of such an impurity atom in a Group 4 lattice. A comparatively small amount of energy is required to remove this fifth electron to the conduction band; for instance, in the case of silicon an energy of ·05 electron volts is required to transfer

* Lecturer in Experimental Electricity, College of Aeronautics, Cranfield.

† Or, as it would usually be described, Q is the minimum amount of energy required to move an electron from the valence band to the conduction band.

this electron to the conduction band compared with 1·1 electron volts required to remove the valence electrons of the silicon atom to the conduction band. Thus at a temperature of absolute zero the contribution to electrons in the conduction band from the impurity atoms is zero, hence the material is still an insulator at absolute zero. A very small increase in temperature, or energy of any form, can however provide the necessary energy to raise the fifth electron to the conduction band. FIG. 4 shows how the number of electrons varies with temperature in an intrinsic crystal and the crystal containing a small amount of impurities. It should be noted that very little increase in temperature transfers nearly all the spare electrons from the impurity atoms of the conduction band; increasing the temperature thereafter increases the contribution of electrons to the conduction band from the lattice itself until the latter electrons predominate over those contributed by the impurity atoms. The difference between the conductivity of intrinsic and impure (or degenerate) semiconductor material at exalted temperature is very small. Thus the electrical properties of semiconductors depend not only on the number of impurity atoms per cubic centimetre but on the energy given to the crystal. Impurity atoms from Group 5 elements are called donor atoms and the material produced by adding donor atoms to intrinsic material is called *n*-type because the mobile carriers are negatively charged.

If elements from Group 3 are used to dope the intrinsic crystal there is a lack of electrons in the structure, or as is usually described there are positive holes associated with the impurity atoms.* Impurity atoms from

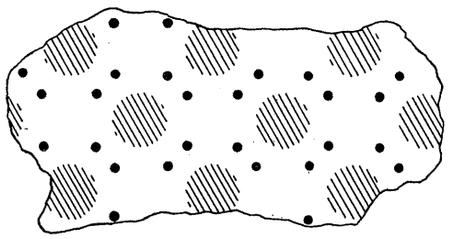

Fig. 1.—Plane diagram of a crystal lattice of an intrinsic semi-conductor

• VALENCE ELECTRONS
NUCLEUS AND LOW ENERGY ELECTRONS

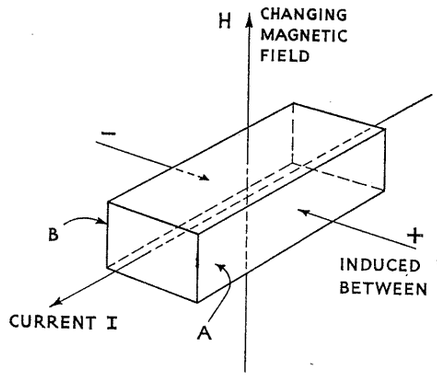

Fig. 2.—The Hall effect in a crystal of semi-conductor material

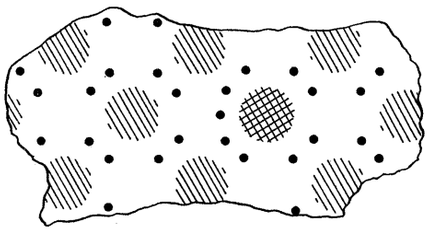

Fig. 3.—Plane diagram of a crystal lattice of semi-conductor material with one atom present from Group 5

• VALENCE ELECTRONS
NUCLEUS & LOW ENERGY ELECTRONS OF GROUP 4 ATOMS
NUCLEUS & LOW ENERGY ELECTRONS OF GROUP 5 ATOMS

Group 3 are called acceptor atoms and the resultant doped intrinsic material is called *p*-type because the mobile carriers behave as if they were positively charged.

It is interesting to note that if an alloy is made with equal numbers of atoms of a Group 3 element and a Group 5 element, then the crystal so produced has the same structure as the Group 4 crystals. Two of these alloys, indium antimonide and gallium arsenide, have been produced and are of great interest.[2] Indium antimonide has an electron mobility of 60,000 cms. per second in a field of 1 volt per centimetre and thus displays a very large Hall effect. Group 4 intrinsic semiconductor material is not very useful except as a means of measuring large changes in magnetic fields or as a thermal detector. However indium antimonide can be used to detect changes in magnetic fields as low as 5×10^{-4} oersteds.[3] One possible use of such a property is for geological survey where the presence of minerals locally distorts the earth's field, thus it might be possible to carry out geological surveys from an aircraft by using an indium antimonide detector.

The *p-n* junction

FIG. 5 shows the distribution of donors and acceptors, and the holes and electrons associated with the impurity atoms in the neighbourhood of a junction between *n*- and *p*-type material.The remaining crystal lattice structure is not shown. In the transition between the two types of material there are no holes or electrons. The junction region can be thought of as a thin slice of intrinsic material between two pieces of degenerate semiconductor material, in other words an elementary capacitor which also of course at all but at absolute zero temperature has a finite resistance. The effect of varying the applied external voltage to the *p-n* junction is shown in FIG. 6 the width of the transition region varying with voltage. Thus both the capacitance and conductivity of a *p-n* junction varies with applied voltage.[4]

The Junction Rectifier

In many aircraft electrical power is produced in the form of a.c. and to convert this to d.c. or to other frequencies a rectifying device is usually employed. Selenium type rectifiers are used in most aircraft installations at the moment but they are not very efficient and even with aluminium cooling fins, forced cooling must be used.

The effect of variation of the conductive properties of a *p-n* junction with the polarity of the applied voltage implies that such a device can be used as a rectifier. FIG. 7 compares the current voltage properties of two power rectifiers, a selenium rectifier and a germanium junction diode. TABLE I compares the properties of both, and from an aircraft point of view the *p-n* junction shows how superior it is in almost every respect, in particular its efficiency and power to weight ratio.

TABLE I

	Efficiency when used as a bridge rectifier	Max. ambient operating temperature	Power/weight ratio Kilowatts/pound
Germanium Junction Diode	77%	55°C.	5·5*
Selenium Rectifier	67%	55°C.	1†

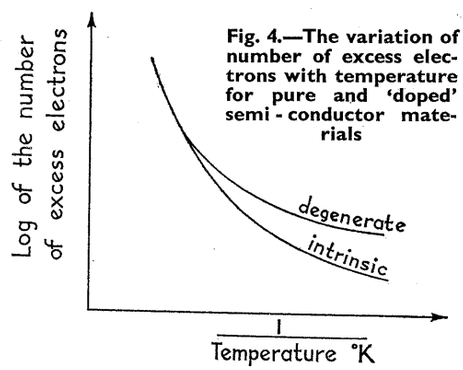

Fig. 4.—The variation of number of excess electrons with temperature for pure and 'doped' semi-conductor materials

Like selenium, the electrical properties of a *p-n* junction deteriorate as its temperature increases as one might infer from the fact that the conductivity of semi-conductors changes with temperature (as shown in FIG. 4). In common with selenium rectifiers *p-n* junction diodes are almost indestructible mechanically (i.e. they can withstand accelerations several hundred times that of gravity without deteriorating). Silicon is superior to germanium in its thermal properties and can operate with the same sort of efficiency up to a temperature of 170 deg. C., which is as good as most known rectifying devices. It would appear then that for most aircraft and missile applications silicon junction diodes will eventually replace the existing low voltage rectifying systems.

The Nuclear Battery

If transistors and similar low powered electrical devices are to be used in aircraft or missiles, particularly when they may have to be stored for months or years without servicing and then brought into immediate

* It is usual to differentiate between movement of holes and electrons because although electrons participate in the transfer of current in both cases the mechanism is entirely different.

* With cooling fins in free air.

† With cooling fins and 2,500 ft. of air blown through the plates/min.

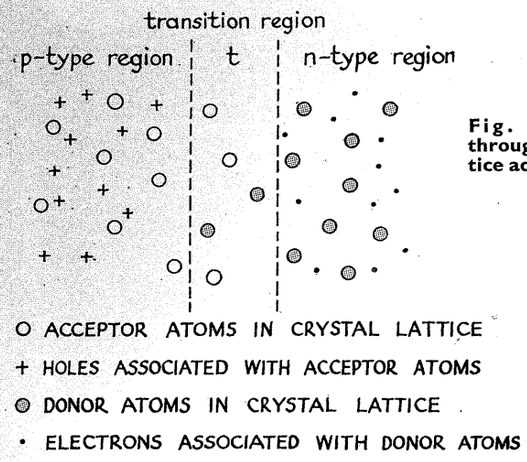

Fig. 5.—A section through the crystal lattice across a *p-n* junction

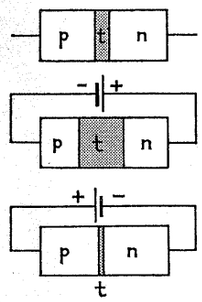

Fig. 6.—The variation of the width of the transition region with applied voltage

Fig. 7 (below).—The current/voltage characteristics of a germanium junction diode and a selenium rectifier

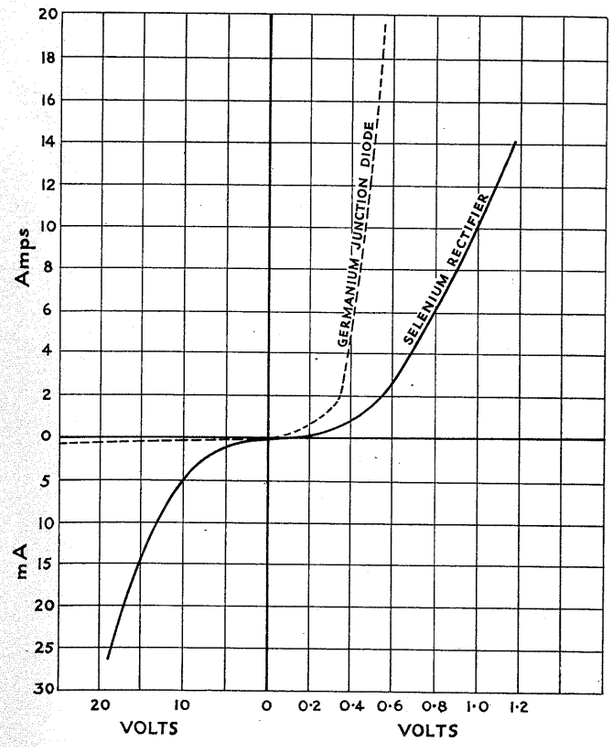

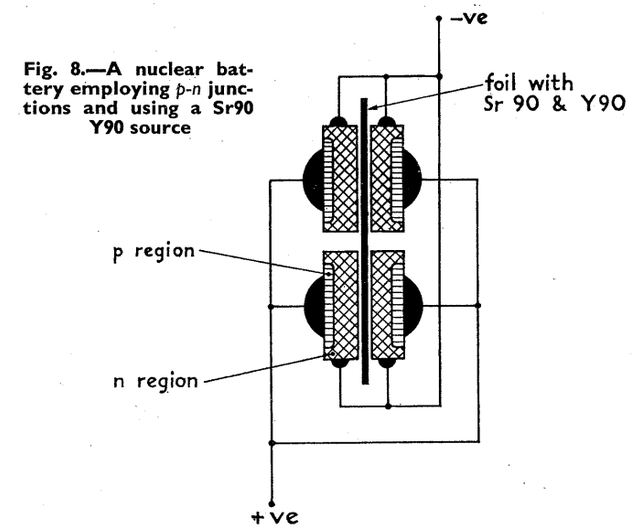

Fig. 8.—A nuclear battery employing *p-n* junctions and using a Sr90 Y90 source

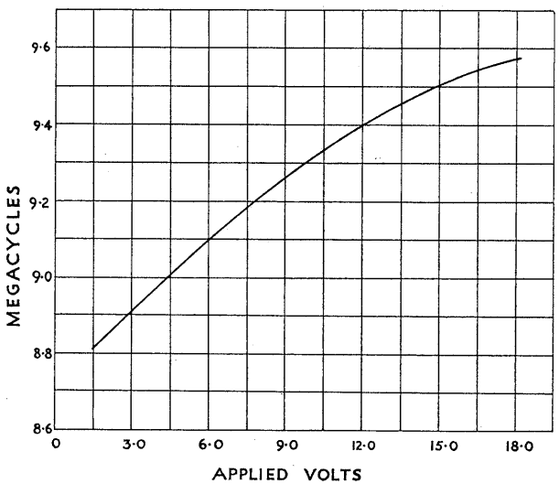

Fig. 9 (right). — The change in frequency produced by varying the voltage applied to a *p-n* junction, which is placed across a parallel tuned circuit

action, the problem of providing power supplies becomes acute because of the deterioration of conventional batteries with storage. Recent investigations into the direct conversion of radioactive energy into electrical energy by using *p-n* junctions have been very encouraging. Transistors do not require much energy to make them operate as small signal devices because they do not require heater supplies as conventional valves do, thus quite small power supplies are sufficient and the 'nuclear battery' can provide this power.[5] If the *n*-type region of a *p-n* junction is bombarded with radioactive particles then electron-hole pairs are generated by ionizing collisions, most of the holes diffusing into the *p*-type region if the thickness of the *n*-type region is less than the critical diffusion length. If it is in excess of the diffusion length then the number of holes reaching the intrinsic region without recombining is small. Thus a voltage is induced across the junction proportional to the energy received from the source. The efficiency of the conversion of radioactive to electrical energy for β particles can be as high as 5 per cent. α particles would be more efficient than this because of their greater specific ionization, but they tend to cause too much damage to *p-n* junctions. Thus if a strip of radioactive material is placed near a *p-n* junction then the latter behaves as a source of electrical energy and can be used as a battery whose storage life is dependent on the half life of the radio-active material. In the case of a mixed source consisting of strontium 90 and yttrium 90 the half life is 20 years. FIG. 8 shows the experimental arrangement of a nuclear battery which has been developed and which can deliver sufficient power to operate a three-stage transistor radio receiver.

Frequency Modulation

The fact that the capacitance of a *p-n* junction varies with applied voltage means that if suitably arranged in a circuit the *p-n* junction can be used as a variable reactance device producing frequency modulation or automatic frequency control. If the device is arranged to produce a change in capacitance without change in resistance with varying applied voltage then very good frequency modulation can be achieved.[4] FIG. 9 shows the change in oscillator frequency with applied voltage of a typical system.[6]

The *p-n-p* Junction

The *p-n-p* junction (or the *n-p-n*) is usually called the transistor and these semiconductor devices have been available for some years in germanium, and silicon transistors have been available for some time in the U.S.A. The *p-n-p* junction can be considered to be two *p-n* junctions back to back, the common *n*-type region being called the base. If one of the *p-n* junctions, called the emitter, is biased so that it conducts and the other *p-n* junction, usually called the collector, is biased so that it does not conduct, then the configuration can behave like an amplifier to current signals applied to the emitter.[7] As well as behaving like conventional valves by amplifying signals, transistors can also be used as oscillators and almost any of the waveform generators.[7,8,9] There is a theoretical upper frequency limit of 3,000 megacycles at which transistors can be operated, which is the sort of frequency that most radar systems use. This has not been achieved in practice but 300 megacycles have been reached, a frequency which is suitable for V.H.F. communication work and telemetering purposes. At the moment it does not seem possible to obtain much power from transistors at high frequencies, thus in any high powered transmitter

conventional valves will always have to be used for the final output stage.

Germanium transistors, like germanium diodes, deteriorate rapidly with increase in temperature and at temperatures much above 70 deg. C. become useless. Silicon transistors, however, like silicon diodes, are capable of operating up to quite high temperatures. For aircraft use the silicon transistor offers many advantages over the conventional valves for radio, radar, computers and other electronic aids at low power levels, and it should replace all conventional valves where low power consumption, small space, and robustness, are required.

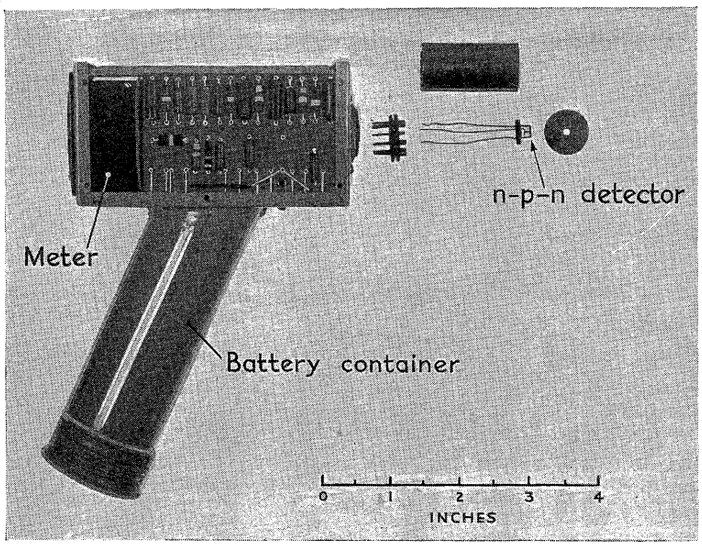

Fig. 10.—The portable radiation monitor showing an exploded view of the plug in detector

A Radiation Detector

In the not too remote future when nuclear reactors are powering aircraft and nuclear weapons are being carried, the radiation hazards to the crew could be very great, particularly as the amount of screening would have to be severely limited because of weight considerations. In a nuclear powered aircraft it is desirable to monitor continuously not only the crews' quarters but the state of the reactor itself. A transistor can be made into a very sensitive detector of α particles because of their high specific ionization.[10] If the base-collector region of a transistor is bombarded with high energy α particles then the quantum yield of electron-hole pairs is considerably enhanced, and quite a large current pulse results from each α particle which arrives within the critical diffusion distance from the collector. This current pulse can be amplified and made to operate a meter which gives an indication of the strength of the source being investigated.

The state of activity of a reactor can be determined by the intensity of the slow or thermal neutrons and if one of the isotopes of boron, B^{10}, is bombarded with thermal neutrons then high energy α particles are emitted.[11] Thus if a boron screen is placed in front of a transistor the device can be used to detect thermal neutrons; hence using such a detector head the state of activity of the reactor can be monitored. If it is required to detect fast electrons a paraffin or polythene moderator can be used to convert the fast neutrons to thermal neutrons before allowing them to fall on the detector. By using its photosensitivity the transistor can also be used to detect β or γ rays if a scintillator is placed in front of the detector in a light-tight enclosure.

FIG. 10 shows a photograph of a portable monitor developed in the Electrical Engineering Department of the College of Aeronautics.[12] It is completely self-contained including its battery supplies and as it is completely transistorized, the power consumption is so small that the device will operate continuously for the duration of the shelf life of the batteries.

Should it be required, the detector head could be some distance from the amplifier and meter so it is possible to have remote monitoring of the reactor or any part of the aircraft.

Thus it can be seen that semiconductor devices, even though at the moment in their infancy, have tremendous potentialities, potentialities which the aircraft industry cannot ignore.

Conduction of Heat within a Structure subjected to Kinetic Heating

A Study of the Problem of Skin Temperature at Hypersonic Speeds

By T. Nonweiler,* B.Sc., A.F.I.A.S.

MANY hold the view that the attainment of very high speeds of flight will be prohibited by the excessive skin temperatures involved, particularly in the vicinity of the wing leading edge, at least until that time when unforeseen advances in metallurgy, or in the application of ceramics, enable the extraordinary problems involved to be overcome. As an opinion it may for all one knows be justified by the event, but it seems (at least to the author) to exaggerate the facts, because it surely ignores the important role played by the conduction of heat along the skin in limiting the temperature. It is the intention of the present article to convert others to this way of thinking.

Of course what is an 'excessive' temperature is open to individual interpretation, and even present-day flight speeds involve heating problems which are difficult enough to solve. This latter remark applies not only to the practical details of structural design, but to the calculation of the temperature distribution within the structure as well, which is part of our present concern. A number of different physical processes of heat transfer are involved, and they are inter-related in such a way that it is difficult to isolate the effect of one apart from all the others, as we must do here.

Of course, to solve any particular problem in detail one has 'simply' to gather together the best of the existing data on all the various properties involved, and feed them into the equations which govern the mechanism of heat transmission, For instance, if the amount of heat transferred from the air to the structure were known, then the relevant equation governing the temperature distribution within the structure is a partial differential equation, involving space variables and perhaps a time variation as well; this in itself is often difficult enough to solve. But the heat transferred from the air is *not* usually known; for the flow in the boundary layer depends on the surface temperature over the body with which it is in contact, not only in the immediate vicinity of the part of the structure under consideration but, to a greater or less extent, everywhere else as well; moreover, except in a few simple conditions, it is very difficult to determine the precise form of this dependence. Thus the aerodynamic heating can only be quoted in intricate and obscure terms of a detailed part of the solution sought, and the complexities resulting from this consideration can best be left to the imagination.

* Senior Lecturer in Theoretical Aerodynamics, College of Aeronautics, Cranfield.

REFERENCES TO LITERATURE

(1) M. R. Wilde. *A relaxation solution in the theory of the compressible laminar boundary layer with variable wall temperature.* (College of Aeronautics Thesis) (unpublished). 1956.

(2) Y. H. Kuo. 'Viscous Flow along a flat plate moving at high supersonic speeds.' *J. Ae. Sci.*, Vol. 23, No. 2. 1956.

(3) L. Lees. 'Influence of the leading-edge shock wave on the laminar layer at hypersonic speeds.' *J. Ae. Sci.*, Vol. 23, No. 6. 1956.

(4) T. Nonweiler. *The laminar boundary layer in slip flow.* (College of Aeronautics Report No. 62.) 1952.

(5) T, Nonweiler. *Surface conduction of the heat transferred from a boundary layer.* (College of Aeronautics Report No. 59.) 1952.

(6) C. J. Smithels. *Metals Reference Book.* (Butterworths.) 1st Ed. 1949.

(7) L. Crocco. 'Lo Strato Limite Laminare nei gas.' *Monografie Scientifiche di Aeronautica No.* 3. 1946.

(8) A. D. Young. 'Skin Friction in laminar boundary layer in compressible flow.' *Aeronautical Quarterly*, Vol. I, Part II. 1949.

(9) T. Nonweiler. *Two-dimensional laminar boundary layer at hypersonic speeds.* (College of Aeronautics Report No. 67.) 1953.

(10) T. Nonweiler. *Heat Transfer over Inclined Wedges at Extreme Skin Temperatures and Speeds.* (College of Aeronautics Report No. 105.) 1956.

(11) R. B. Erb. *The effect of conduction of heat within a body on temperature distribution and rate of heat transfer.* (College of Aeronautics Thesis.) (Unpublished.) 1954.

It would not do, however, just to raise one's hands in horror and admit, quite honestly maybe, that the problem is intractable! As those hands have often belonged to aerodynamicists, who are long practised in the craft of making assumptions and simplifications, it is not surprising that they have solved the problem in various degrees of approximation. This practice has led to the recognition that under certain conditions it is quite reasonable to ignore certain factors, and construct numerical solutions with fair accuracy, though often only after tedious computations.

The Result of ignoring Skin Conductivity

One of these factors most commonly ignored is the effect of the conductivity of the skin on its temperature distribution: or more exactly, the rate of heat transfer within and parallel to the heated surface. Bearing in mind that the whole problem is so complicated, it may seem unnaturally perverse to discuss just this one, apparently small, effect in the present article. Yet we shall try to show that, under certain circumstances, its consideration is all-important in setting limitations on the temperature rise

due to kinetic heating. Admittedly these circumstances arise only in conditions of flight at such extreme speeds that they are of little interest in aircraft design today, but they are certainly relevant to the problems of tomorrow, when aircraft or missiles may suffer heating to such an extent that its limitation is likely to be one of the main features of the aerodynamic design. But in view of the complex nature of the problem, of which we shall be studying one small part, the reader will no doubt be prepared to accept some rather sweeping assertions and simplifications, which are thereby made necessary if the essential points of the argument are to emerge.

For a start, we shall consider a two-dimensional structure, shaped as a thin, hollow shell (FIG. 1), over the outside of which the air is moving at speeds so high that the kinetic heating effect is appreciable: this simulates the problem of heat transfer to a wing of stressed skin construction. The general equation for the propagation of heat in the conducting medium of the shell simply states that the rate of heat conduction into any element of volume equals the rate at which that element gains heat. If we apply this principle to an element formed as a small strip of the wing skin, cut off perpendicular to its exterior surface, and assume that the conduction along the skin (i.e. through the sides AD, BC sketched in FIG. 1) can be ignored, then the rate of gain of heat of this element equals that conducted into the exterior and interior surface elements (AB and CD of the figure). It is often appropriate to suppose that the inside surface is insulated: one can easily foresee reasons why this should sometimes be a realistic and desirable feature. This being so, the heat lost from the interior surface CD would be zero, while that through the exterior surface AB is equal to the resultant heat flux transferred from the boundary layer, and due to radiation.

Generally the most important source of radiative heat exchange is that emitted away from the surface, which varies as the fourth power of its temperature, and as the emissivity of the surface. Of course there are sources of heat absorption by radiation from the atmosphere, or the earth's surface and the sun, and these can be estimated, but little point is served by including them in a general analysis. We can sum up by stating that the rate at which the element of skin ABCD gains heat equals the heat transferred from the boundary layer through AB, less that lost by radiation over the same part of the surface.

Ultimately after a sufficient length of time in steady flight, an equilibrium condition would be reached in which the skin no longer gains heat, and this occurs when the skin temperature is such that the heat it radiates equals that transferred from the boundary layer. What length of time is involved before this condition is reached depends on the whole history of the motion: a ballistic missile, like the V2, has a trajectory involving constant and rapid change, so that an equilibrium condition is never reached. On the other hand, the rate of heat transfer from the boundary layer becomes progressively larger towards the nose where the boundary layer is thinnest; consequently the more rapidly in this region does the skin temperature reach its equilibrium value.

Heat Transfer at the Nose

In fact, all the simple theories of boundary layer flow show that, unless the surface temperature has a local value known as the 'thermometer' temperature, the heat transfer at the nose is infinite; consequently the temperature actually at the nose becomes immediately equal to the thermometer value, at least if what we have so far asserted is true. These assertions are in fact those usually accepted, and a typical temperature distribution[1] calculated in this way is shown in FIG. 2. But applied to surfaces moving at very high speeds this kind of argument leads to some rather alarming deductions.

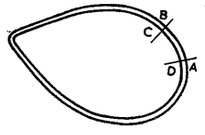

Fig. 1

The thermometer temperature rise at the nose (where the boundary layer is laminar, and where, in supersonic flow, the air outside the layer has a finite speed) is roughly about 85 per cent of the stagnation temperature rise, which in turn equals $(V/100)^2$ degrees Centigrade, if V is the speed of the wing relative to the undisturbed air, measured in m.p.h. At a speed of 10,000 m.p.h. corresponding perhaps, to a Mach number of about 15, evidently the thermometer temperature would be around 10,000 deg. C.! Is it really true that flight at such speeds inevitably involves such fantastic skin temperatures?

Fortunately for the aspiring spaceman, the answer is in the negative. Something has gone wrong with the argument, and one has to examine critically the assumptions which lead to this result. Apart from those specifying the nature of the problem, which we have to take for granted, the two assertions that come under suspicion are:

(*i*) that the conduction along the skin is negligible; and

(*ii*) that the heat transfer at the nose is infinite (unless the surface has the thermometer temperature).

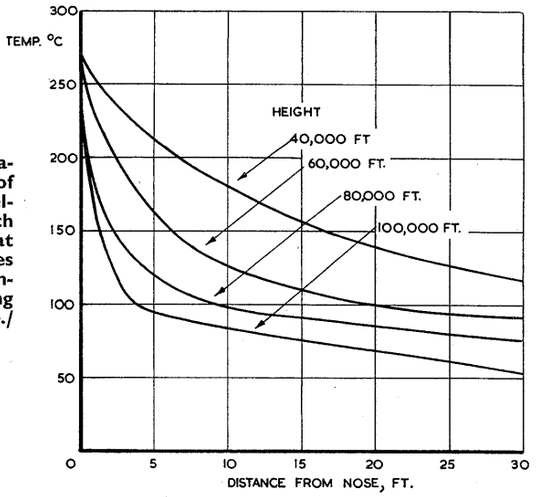

Fig. 2.—Temperature over wing of an aircraft travelling at a Mach number of 3 at various altitudes (neglecting conductivity) (Wing loading = 60 lb./sq. ft.)

Of course it is no secret that the former assumption will come under close scrutiny in the present discussion. But it would be wrong to pretend that the second assertion is faultless. The heat transfer at the nose is almost certainly finite, though what value it has there is very difficult to find.

In all fairness to the problem under primary consideration, we can hardly leave this other matter without further amplification. Supposing that the boundary layer flow is laminar, which must certainly be true of the immediate vicinity of the nose, the assertion (*ii*) above can readily be proved for the supersonic flow past a sharp-nosed wing, subject to the usual boundary layer approximations. Unfortunately, all these approximations break down in the region of the nose. For a start, the simplified form of the Prandtl equations of motion for the flow are no longer valid: one should use instead the full Navier Stokes equations for a viscous fluid which have, however, so far defied solution. Quite apart from this, particularly at high Mach number, the displacement effect of the boundary layer introduces significant longitudinal pressure gradients[2]; there are as well interactions between the nose shock wave and the boundary layer which have some effect[3]. As yet, however, it has not been found whether such considerations show a limit to the rate of heat transfer, though they certainly limit the intensity of skin friction. Again, the commonly made assumptions of no slip, and of no temperature difference between the air at the surface and the surface itself, are not strictly true, and even if the actual amount of slip and temperature jump are minute, they can cause a slight reduction in heat transfer, which becomes progressively more important towards the nose[4]. Although indeed maximum values of heat transfer can be deduced on this basis, little credence can be attached to these calculations, which implicitly assume that the reduction is small.

In view of these obscurities, we shall retain the assumption that the heat transfer at the nose is infinite; in fact we shall suppose the usual 'flat plate' result, that it goes to infinity like $1/x^{1/2}$, where x is the distance from the nose. Plainly if we are seeking to find a limit to the nose temperature—imposed by the conduction of heat within the skin—this is a pessimistic assumption, because it over-estimates at least the local rate of heat transmission.

The Effects of Skin Conductivity

Certainly the conduction of heat does have an important effect on skin temperature distribution. We can quite readily see why this is by referring back to results, like those shown in FIG. 2, derived on the basis of its neglect. Although the nose temperature is then the thermometer temperature, and therefore varies as the square of the speed, the equilibrium skin temperature further downstream is dependent on a balance of the boundary layer heat transfer with the radiation from the surface; the former reduces

Notation

L_m	Wing loading (Kg./sq. m.)
$Q/x^{1/2}$	Rate of heat flux per unit area to surface from boundary layer (Q assumed independent of x)
T	Temperature (deg. C. absolute)
T_{max}	Maximum temperature (at leading edge)
V	Speed of flight
d	Skin thickness
d_m	Skin thickness (mm.)
k	Skin conductivity
k_m	Skin conductivity (cal./cm./sec./deg. C.)
l	characteristic length of surface affected by conductivity
p	air pressure outside boundary layer (atmospheres)
x	distance along surface from leading edge
α	semi-nose-angle of solid wedge
ϵ	skin emissivity
σ	Stefan's constant ($5{\cdot}7\times10^{-12}$ watts/sq.cm./sec./deg. C^4).

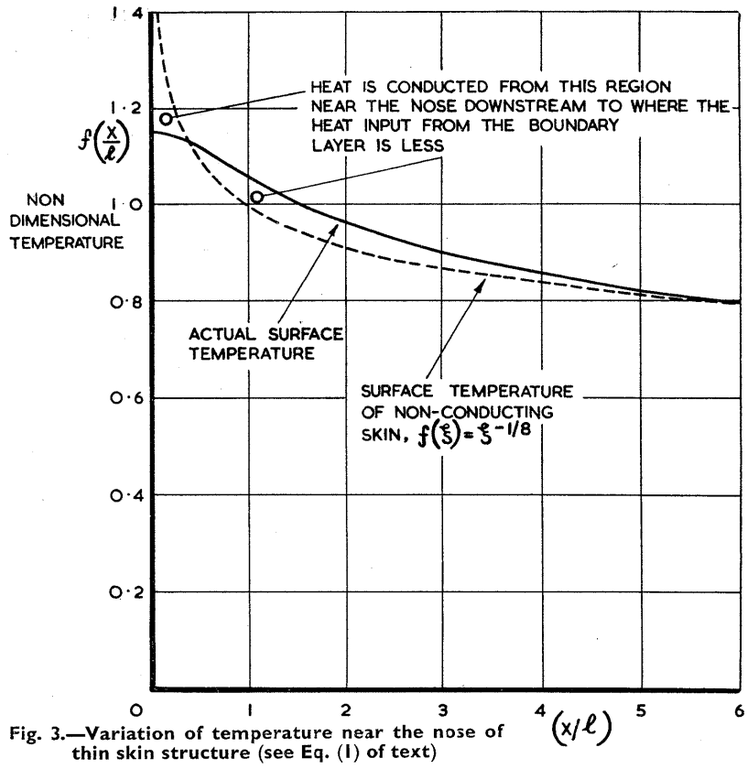

Fig. 3.—Variation of temperature near the nose of thin skin structure (see Eq. (1) of text)

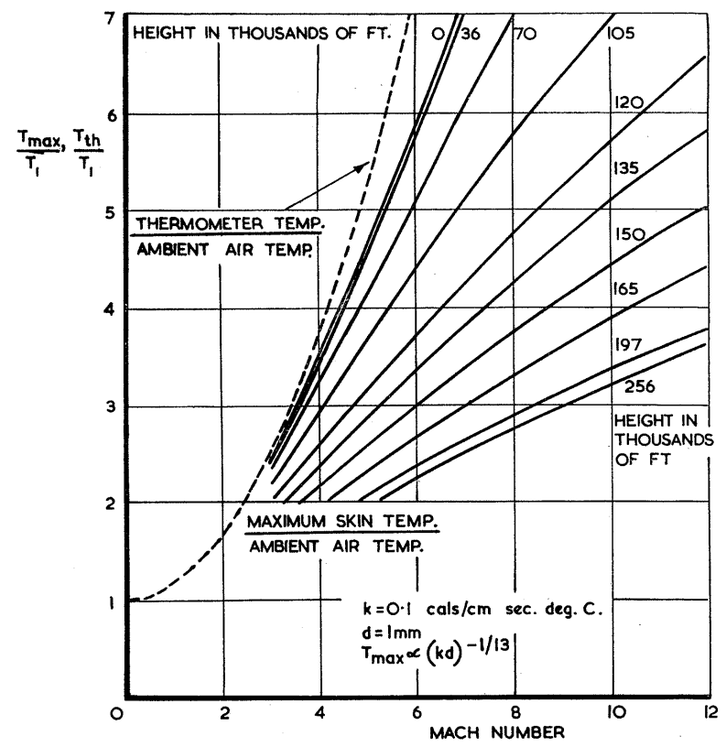

Fig. 4.—Variation of maximum skin temperature with flight Mach number and height, for a flat plate behaving as a perfect black body emitter on the outside and insulated on its inner surface (N.A.C.A. standard atmosphere assumed)

with decreasing air density at high altitudes, but the latter does not. For example, the heat transfer (at high speeds) from a laminar boundary layer at a fixed distance downstream of the nose, varies roughly as the square of the speed, and the square root of the air pressure (p); on the other hand the radiation varies as the fourth power of the skin temperature (T). Thus for the two to be equal, we find that downstream of the nose

$$T \propto p^{1/8}\, V^{1/2}$$

However crude this approximation may be, it does draw attention to the fact that either as the altitude or speed is increased, and of course they are frequently increased in conjunction, the ratio of the nose (thermometer) temperature to that downstream becomes accentuated. Consequently, the temperature gradient along the skin is also accentuated.

Fig. 5 (right)

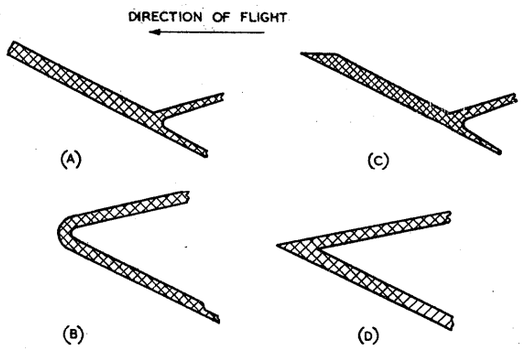

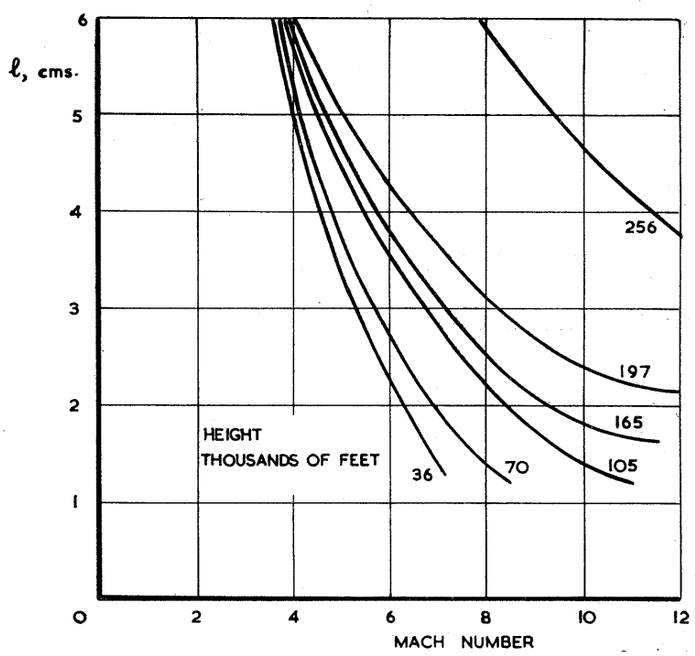

Fig. 6.—Variation of characteristic length of surface, l, for a thin skin structure (k=0·1 cal./cm./sec./°C., d=1 mm.)

The effect of increase in altitude in causing this is certainly evident from FIG. 2; the effect of increase in speed would be even more apparent. Furthermore, if the skin is still heating up to its equilibrium value, the rate of increase of temperature towards the nose would be yet more marked.

Now, the longitudinal rate of heat conduction (per unit span) equals

$$kd\frac{\partial T}{\partial x}$$

where k is the thermal conductivity of the skin, d is its thickness, and $\partial T/\partial x$ is the longitudinal temperature gradient. Its neglect might therefore be justified if the skin was sufficiently thin, and in relation to the performance and construction of existing aircraft, this is usually so. But if the structure is to be used on a very high speed craft, or one operating at extreme altitudes, we have just indicated that the longitudinal temperature gradient (found by neglecting heat conduction) becomes very large close to the nose. So large, in fact, that it is a gross simplification to ignore the amount of heat being transmitted along the skin (away from the nose), compared with that transferred from the boundary layer, or radiated from the surface. This conduction will modify the skin temperature by effectively cooling the region near the nose, and heating it downstream, relative (that is) to conditions in a non-conducting skin.

Some calculations of its precise effect have been attempted, and although no complete derivation of the relevant equations[5] will be stated here, a summary of the assumptions made is of relevance:

(*i*) the skin is taken as of uniform thickness, d;

(*ii*) the rate of heat input per unit area from the boundary layer is treated as equal to $Q/x^{1/2}$, where Q can be taken as a constant over that part of the surface sensibly affected by conduction, whose characteristic length is l, say;

(*iii*) the ϵmissivity of the exterior skin surface is ϵ;

(*iv*) the inner surface gains or loses no heat either by conduction or radiation;

(*v*) steady flight conditions exist so that close to the nose we may ignore the variation of temperature with time;

(*vi*) the skin thickness is so small that the temperature within the skin does not differ greatly from that on its exterior surface; this implies that d must be small compared with the characteristic length, l.

The dimensional quantities involved in the problem are

$$d,\ Q,\ x,\ T \text{ and } k,$$

which have already been defined, together with Stefan's constant, σ. Dimensional homogeneity shows that the functional relation for the temperature will take the form:

$$T=(k/\sigma d)^{1/3} f(\sigma d^{5/2} Q^3/k^4,\ x/d,\ \epsilon)$$

In fact, it is more simple than this, as the terms k and d only occur together as a product, in the expression for the heat conducted along the skin; and likewise ϵ only appears in conjunction with Stefan's constant, σ, in the term representing the radiation away from the skin. It is not difficult to deduce as a result that the relation has the more specific form:

$$T=(Q^4/kd\epsilon^3\sigma^3)^{1/13} f(x/l) \quad \text{where } l=(k^4d^4/\epsilon\sigma Q^3)^{2/13} \quad \ldots\ldots\ldots \quad (1)$$

The appearance of a thirteenth root in a physical law is certainly rather remarkable, but there it is.

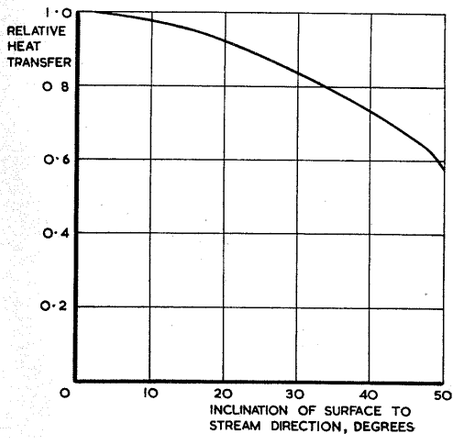

Fig. 7.—Rate of heat transfer per unit area on a forward facing inclined plane surface relative to that of flat plate at zero incidence subjected to same surface pressure and moving at same speed (no results available beyond an angle of 50° where leading-edge shockwave becomes detached)

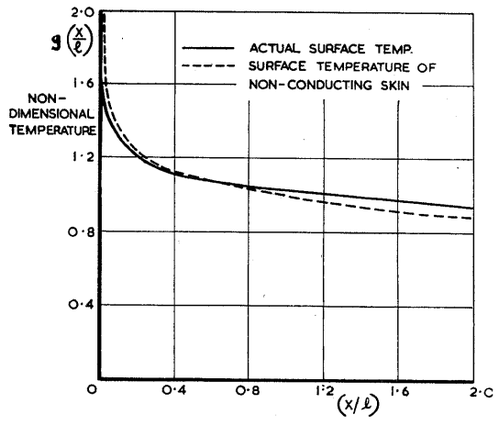

Fig. 8.—Variation of temperature near the nose of a solid wedge (see Eq. (4) of text)

Some Calculated Results

The variation of the function f is shown in FIG. 3, together with the curve

$$T=(Q^4/kd\epsilon^3\sigma^3)^{1/13}(l/x)^{1/8} \quad \text{or } \epsilon\sigma T^4=Q/x^{1/2}$$

representing the condition of zero nett heat transfer into the surface, to which it is asymptotic. In other words, far enough downstream from the nose, the heat flux, not only into, but also along, the skin tends to zero, and can indeed be ignored, as we have been led to suggest before. Relative to this condition, the effect of conductivity is also what we have already anticipated, and the maximum value of skin temperature is reached at the nose where

$$T_{\max}=1\cdot15\ (Q^4/kd\epsilon^3\sigma^3)^{1/13} \quad \ldots\ldots\ldots\ldots\ldots\ldots\ldots\ldots \quad (2)$$

The maximum temperature gradient is also of interest, and this is determined by the maximum value of $f'(\xi)$ to be

$$(-\partial T/\partial x)_{\max}=0\cdot13\ \ (Q^{10}/k^9d^9\epsilon\sigma)^{1/13}=0\cdot11(T_{\max}/l) \quad \ldots\ldots\ldots \quad (3)$$

Without putting any numerical values in these formulae, we can at least observe the following qualitative effects: namely, that if either

(*i*) the heat transfer from the boundary layer is increased (i.e. the altitude is lowered, or the speed increased),

(*ii*) the skin conductivity is decreased, or

(*iii*) the skin thickness is decreased,

then

(*i*) the temperature is increased,

(*ii*) the temperature gradient is increased, and

(*iii*) the region affected by conductivity is decreased (this is a multiple of the characteristic length, l).

Obviously the precise magnitude of the effects varies quite considerably: for instance the skin temperature is relatively insensitive to skin thickness and conductivity as such, but the temperature gradient is influenced by these properties to a much greater extent. One property whose effect is unusual is the surface emissivity; if this is reduced both the skin temperature and temperature gradient increase but so also does the extent of the surface over which conductivity appreciably modifies the temperature distribution.

To obtain some idea of the actual numerical values involved, we shall have to commit ourselves to some estimate of the boundary layer heat transfer. This can be reasonably attempted however without a precise knowledge of the downstream surface temperatures, because conditions at, or close to, the nose are dependent only on the surface temperature of the nose; thus the value of Q can consequently be calculated for various flight speeds and altitudes, as if the surface had a uniform temperature $T_{\max}$; Eq. (2) can then be used to give the maximum surface temperature. Eqs. (1) and (3) subsequently yield the characteristic length of surface over which conductivity is important, and the temperature gradient. For simplicity, 'flat plate' values of heat transfer calculated on this basis have been used to compose FIGS. 4 and 5, together with the arbitrary assumptions that $\epsilon=1$, and

$$k=0\cdot1 \text{ cals./cm. sec. deg. C}, \qquad d=1 \text{ mm.},$$
$$=24\cdot2 \text{ B.Th.U./ft. hr. deg. F}, \qquad =0\cdot0394 \text{ in.},$$
$$\text{i.e. } kd=0\cdot0418 \text{ watts/deg. C.}$$
$$=3\cdot11\times10^{-5} \text{ h.p./deg. F.}$$

Some reasonable idea of the change to be expected from different values of ϵ, k and d can be readily obtained from the formulae already quoted. The conductivity figure is typical of alloy steel. An indication of the effect of using an equal thickness of a different material[6] is given by the data of TABLE I; the figures quoted are based on the conductivity at ordinary temperatures; for most pure metals its value decreases with temperature, though the reverse appears true of alloys.

The use in these figures of zero incidence 'flat plate' values of heat transfer is convenient, but of course it must be remembered that the compression behind the nose shockwave can be quite severe and modify the result appreciably. In the numerical calculation of heat transfer the data of Refs. 7 and 8 have been invoked.

A Limit to the Skin Temperature at Extreme Speeds

The actual values in the limiting case of large Mach numbers (beyond 10) are not without interest, at least in relation to long-range ballistic missiles, or even spaceships. In this condition it can be shown[9] that the rate of heat transfer to a 'flat plate' is asymptotic (from below) to the value

$$Q/x^{1/2}=1\cdot09\times10^{-3}V^2\sqrt{(p/x')} \text{ ft.lb./sq.ft./sec.}$$
$$=440\times10^{-5}V_m^2\sqrt{(p/x_m)} \text{ Kw./sq.m.}$$

where V (or V_m) is the flight speed in m.p.h. (or metres/sec.), p is the air pressure outside the boundary layer in atmospheres, and x' (or x_m) is in ft. (or metres). Quite clearly a lifting wing on such a high-speed missile is going to be hotter on its underside, where the pressure is higher. Now the pressure on this side, in level flight, must at least be equal to the wing loading due to lift: it will indeed be more than this unless the pressure over the upper surface is negligible, and the underside is flat. Local reductions in pressure below this value can of course be produced near the nose by making the underside concave, but for one thing the formulae quoted assume no pressure gradient and are therefore incapable of predicting the resulting change in heat transfer; and for another compressive supersonic flows are generally to be avoided, due to the obscure forms of shock wave and boundary layer interactions thereby produced.

Remembering that the lift needed is effectively reduced at the kind of speeds we have in mind by the centrifugal force in circling about the earth at constant height, it is not difficult to show on this basis that the heat transfer, and so the skin temperature, will reach its maximum at about the speed where pV^4 is a maximum, and where (if R is the earth's radius) the pressure p varies $\{1-(V^2/gR)\}$. This maximum occurs where

$$V^2=2gR/3$$
$$\text{i.e. } V=14{,}500 \text{ m.p.h.}$$
$$\text{or } V_m=6{,}460 \text{ metres/sec.}$$

Interpreting the pressure in terms of the wing loading in this way, it follows that the highest value of the rate of heat transfer, which is reached in sustained flight at about this speed, is therefore

$$Q/x^{1/2}=10\cdot5(L_m/x_m)^{1/2} \text{ Kw./sq.m.}$$
$$=2{,}860\ (L'/x')^{1/2} \text{ ft.lb./sq.ft./sec.}$$

where L' (or L_m) is the wing loading in lb./sq. ft. (or kg./sq. m.).

Using this value in Eq. (2) we find that the highest value of the maximum temperature is

$$T_{\max}=1{,}000\ (L_m^2/\epsilon^3k_md_m)^{1/13} \text{ deg. Abs.}$$

where k_m is in cals./cm./sec./deg. C., and d_m is in mm. Supposing that the chosen wing loading were 100 Kg./sq. m. (20·5 lb./sq. ft.), we reach the rather alarming conclusion that it would need a thickness of several inches of steel to avoid it melting, let alone to provide adequate strength. But before the reader has time to smirk, let us see what can be done to remedy this.

Important reductions in skin temperature can be effected by increasing the emissivity, but of course this is limited above to the 'black-body' value

of unity. Yet we can effect a further reduction by relaxing the assumption that the inner surface of the wing is insulated: supposing that the interior of the wing is hollow and non-conducting, we can nevertheless allow a heat exchange internally by radiation. This can be simulated by increasing the figure for emissivity ϵ, by taking it to give the nett radiative loss from both surfaces of the underside skin. If all surfaces are 'black', half of the heat radiated to the upper side of the wing is returned by radiation from its inner surface, and the other half is conducted through this skin, which is assumed to receive no heat from other sources, and radiated to the atmosphere: thus the total nett loss of heat by radiation from the pressure side of the wing is (roughly) given by taking $\epsilon=1\cdot5$. (Admittedly the upper side surface temperature is thereby increased—but only to a value of $2^{-1/4}=0\cdot84$ of that of the pressure side.)

Better still, we can allow the underside wing surface to project forward of the upper one (FIG. 5a). The radiation from the 'inner surface' (which now becomes the 'upper surface' of the wing) is not now returned, nor is there any appreciable kinetic heating of this side. It is possible once more to allow for this by taking ϵ as the sum of the emissivities of each side of the projection: for 'black' surfaces consequently we can take $\epsilon=2$.

Again, we see that further reductions can be brought about by employing low wing loadings—thereby reducing the heat transfer from the boundary layer because of the lower air pressures. We can take it that there will consequently be a strong incentive for this to be a design characteristic of many hypersonic aircraft—which is an amusing thought, because the tendency is most marked nowadays in relation to the design of very flow speed aircraft.

We have, finally, one more trick up our sleeves. It will be recalled that the wing is assumed flat-sided (wedge-shaped), with negligible pressure on its upper side in level flight. On the other hand, the incidence of the under side will increase with altitude of flight, as higher compression is needed across the leading edge shock wave to supply the required component of lift force. Now the figures quoted earlier for heat transfer at high speeds refer specifically to that over a surface at *small* incidence to the stream. At larger angles, but with the same value of surface pressure and speed of flight, the heat transfer is markedly reduced, as shown by FIG. 6 (from Ref. 10). This is primarily because the speed behind the intense shock wave, and outside the boundary layer, is so much smaller. Making allowance for the increase in pressure required on the underside to produce the same component lift force on the wing, we find that with the lower surface inclined at an angle of 50 deg. to the direction of flight, the heat transfer is reduced by a third of the value we have allotted to it.

Of course, such high incidence as this might conceivably be unwelcome, as it is evident that the (lift/drag) ratio of the configuration is very poor. But the fact does show why it pays to combine extreme speeds with extreme altitudes, because such an incidence would only be achieved by maintaining level flight at such a height that the indicated air speed is kept very low. In fact, with a wing loading of 100 Kg/sq. m. (20·5 lb./sq. ft.) an incidence of 50 deg. (on the lower surface) can be shown to require an I.A.S. of 50 m.p.h., which (at the speeds we have in mind) implies flight at an altitude where the relative density is about 10^{-5}, or say, a height of 50 miles (80 Km.).

Taking account of all these possible sources of reduction, a few sums will soon persuade the reader that the maximum temperature can be kept within very reasonable bounds. Figures of around 1,000 deg. C. (for 0·1 in. thick steel) are all that *need* be involved. Of course we cannot rule out the possibility that transition to turbulent flow within the boundary layer may occur downstream, and with it involve higher temperatures in that region. But here again we must remember that flight at high altitude, together with the attendant high temperatures of the flow behind the intense shock (developed by the wing at high incidence), serves to keep Reynolds numbers low, and increase the stability of laminar flow. Precisely what likelihood there is of the avoidance of turbulence—or indeed its effect, if present—probably no one would care to predict for such extreme conditions as we have in mind.

A Solid Leading Edge

Even if one is forced to the use of a very thick skin to keep the temperature down, such a modification would only be needed in the immediate neighbourhood of the nose; typically over a distance of a few inches. But there are objections to the application of the results we have described in such an eventuality. For one thing, conductivity from one side of the skin to the other is no longer negligible, because its thickness could be appreciable by comparison with the characteristic length, l. For another, either there must be a region of much higher pressure at the nose (FIGS. 3a and b), or else the skin thickness will not remain constant (FIGS. 3c and d), over a length which again cannot be ignored compared with l.

To take some account at least of the latter eventuality, calculations have been attempted to take account of conductivity in a *solid* wing.[11] The same kind of dimensional argument as was used before, now shows that for a solid wedge, which has a small semi-wedge angle α, say, but which has no characteristic length dimension,

$$T=(Q^2/\epsilon\sigma\alpha k)^{1/5}g(x/l) \qquad \text{where } l=(\alpha^4k^4/\epsilon\sigma Q^3)^{2/5} \quad \ldots\ldots\ldots\ldots \quad (4)$$

These forms should be compared with those in Eq. (1), and it will then be seen that the effects of the various parameters involved are qualitatively similar. Identical forms can likewise be obtained for solid cones (or conical shells). The reference work also lists corresponding formulae for a solid paraboloid, and a parabolic nose configuration, but of course the variation of the rate of kinetic heating with distance along the surface on such shapes is very problematical. Moreover, there are reasons peculiar to the differential equations involved why it is particularly difficult accurately to determine a numerical solution, subject to the appropriate boundary conditions.

A tentative estimate of the variation of the function g defined by Eq. (4) is shown in FIG. 7. It is difficult to find any satisfactory basis of comparison between these results and those relevant to a uniform skin thickness, but very much as one might expect, the maximum temperatures are generally rather higher for the solid wedge, owing to the decreasing effective skin thickness towards the nose. The temperature gradient is certainly higher: it is in fact infinite at the leading edge of the wedge. On the other hand, the results are much more sensitive to properties of the material: as will be seen from TABLE I, the use of a good conductor (like copper) can reduce the nose temperature by over a third, by spreading the region affected by conductivity over some 35 times the length of surface, relative to steel. Likewise significant changes can be brought about by changes in the wedge angle.

In the form quoted, these results apply to a wedge with a symmetry in heat transfer characteristics about the plane of symmetry of the wedge; in other words, the wedge is at zero incidence, and has equal surface emissivities on both sides. It is quite easy to adjust for any other condition by replacing α, Q and ϵ in Eq. (4) by 2α, (Q_1+Q_2) and $(\epsilon_1+\epsilon_2)$ respectively, where suffices '1' and '2' denote the values of these properties on the upper and lower surfaces (respectively) of the wedge. For example, in relation to the condition cited earlier of a wing of a hypersonic aircraft subjected to a high rate of kinetic heating on the under side only, we may take $Q_1/Q_2=0$, but if the surface conditions are identical, $\epsilon_1/\epsilon_2=1$; then the temperature is reduced by a factor $1/2^{2/5}$, relative to an otherwise similar condition of symmetry.

But without going over similar ground again, the reader by this time will be left in no doubt that the action of conductivity can limit the skin temperature at the nose to a reasonable value, provided only that the structure is sufficiently thick to enable a sufficient flux of heat along it. Remembering that in all likelihood the values of boundary layer heat transfer we have used are on the large side, there is room one feels for a cautious optimism that the problems of flight at extreme speeds—even at Mach numbers of 10 or 20, do not necessarily imply possibilities. Indeed, it might not be too incautious to remark that these problems appear not very much more difficult than many of those involved in the design of present-day turbine blading for jet engines.

TABLE I

* Assuming $k=0\cdot1$ cal./cm./sec./°C.

† Data refer to temperatures of 100°C.

Metal or Alloy	Melting Point °C.	Thermal Conductivity† cal./cm./sec./°C.	S.G.†	Max. temperature relative to that of steel*		Characteristic length, l, relative to that of steel*		Max. temperature gradient relative to that of steel*	
				of equal thickness	of equal wedge angle	of equal thickness	of equal wedge angle	of equal thickness	of equal wedge angle
Aluminium	660	0·49–0·54	2·71	0·88	0·72	2·7	13·8	0·32	
duralumin	650	0·31–0·38	2·80	0·91	0·78	2·2	7·2	0·42	
Beryllium	1280	0·38	1·82	0·90	0·76	2·2	8·4	0·40	
Copper	1083	0·91–0·95	8·94	0·84	0·64	4·0	35·5	0·21	
brass (70% Cu)	954	0·23–0·29	8·52	0·93	0·83	1·8	4·6	0·52	
phosphor bronze (93/7)	1040	0·16	8·92	0·96	0·91	1·3	2·1	0·72	
Iron	1527	0·18	7·87	0·95	0·80	1·4	2·6	0·66	
mild steel (0·2% C)	1500	0·12	7·87	0·99	0·96	1·1	1·3	0·88	
high carbon steel (0·8% C)	1465	0·12	7·85	0·99	0·96	1·1	1·3	0·88	
stainless steel (13% Cr, high C)	1495	0·06	7·55	1·04	1·11	0·73	0·44	1·42	
stainless steel (18% Cr, 8% Ni)	1470	0·04	8·00	1·07	1·20	0·57	0·23	1·89	
heat-resisting (26% Cr, 10% Ni)	1500	0·03	7·90	1·10	1·27	0·48	0·15	2·30	
heat-resisting (30% Cr)	1450	0·03	7·90	1·10	1·27	0·48	0·15	2·30	
nichrome (60/20/20)	1440	0·03	8·00	1·10	1·27	0·48	0·15	2·30	
Magnesium	649	0·34–0·38	1·74	0·91	0·77	2·2	7·8	0·41	
Molybdenum	2620	0·33–0·35	10·40	0·91	0·78	2·1	7·1	0·43	
Nickel	1455	0·14	8·88	0·97	0·93	1·2	1·7	0·79	
Monel	1350	0·06	8·83	1·04	1·11	0·73	0·44	1·42	
cupro-nickel (70/30)	1230	0·09	8·94	1·01	1·02	0·94	0·84	1·07	
Titanium	1800	0·04	4·50	1·07	1·20	0·57	0·23	1·89	
Wolfram	3382	0·39	19·32	0·90	0·76	2·3	8·8	0·39	Infinite for all materials

Aircraft Engineering
BUNHILL PUBLICATIONS LTD
12 Bloomsbury Square, W.C.1